

Insights into a million-year-scale Rhenohercynian carbonate platform evolution through a multi-disciplinary approach: example of a Givetian carbonate record from Belgium

D. PAS*†, A. C. DA SILVA*, X. DEVLEESCHOUWER‡, D. DE VLEESCHOUWER§, P. CORNET*, C. LABAYE* & F. BOULVAIN*

*Sedimentary Petrology, B20, Université de Liège, Sart-Tilman 4000, Liège, Belgium

‡O.D. Earth and History of Life, Royal Belgian Institute of Natural Sciences, 13 Rue Jenner, B-1000, Brussels, Belgium

§SMARUM—Center for Marine Environment Sciences, University of Bremen, Leobener Strasse, D-28359 Bremen, Germany

(Received 25 February 2015; accepted 21 March 2016)

Abstract—In this paper we formulate answers to three important questions related to Givetian carbonate records and their use for reconstructing million-year-scale past palaeoenvironmental changes. First, we provide detailed illustrations of the fascinating diversity that shaped a significant shallow reefal platform during early to late Givetian time in the Rhenohercynian Ocean; secondly we improve the sedimentological model of the extensive Givetian carbonate platform in the Dinant Basin; and thirdly we evaluate the application of magnetic susceptibility as a tool for long-term trend correlations and palaeoenvironmental reconstructions. These goals are reached by making a sedimentological, geophysical and geochemical study of the La Thure section. Through the early–late Givetian interval we discerned 18 microfacies ranging from a homoclinal ramp to a discontinuously rimmed shelf and then a drowning shelf. The comparison of these sedimentological results with those published for the south of the Dinant Syncline allowed us to provide an up to date model of the vertical and lateral environmental development of one of the largest Givetian carbonate platforms in Europe. This comparison also increased the knowledge on the distribution of facies belts in the Dinant Basin and allowed us to highlight the Taghanic Event. Palaeoredox proxies reveal a substantial change in the oxygenation level, from oxygen-depleted to more oxic conditions, between middle and late Givetian time. We demonstrated the relationship between variation in magnetic susceptibility values and proxies for siliciclastic input (such as Si, Al). The La Thure section is considered a key section for the understanding of internal shelf settings bordering Laurussia's southeastern margin.

Keywords: Devonian, palaeoenvironment, palaeoclimate, sedimentology, magnetic susceptibility.

1. Introduction

The Belgian Givetian sedimentary sequence of the Ardennes area represents one of the thickest and best-known Palaeozoic reef-related deposits of Europe. The relatively large quarries within the Givetian rocks and the numerous valleys crossing the Ardennes area offer easy access to a number of outstanding outcrops, allowing detailed sedimentological, biostratigraphical and taxonomic research (Lecompte, 1951, 1952; Errera, Mamet & Sartenauer, 1972; Bultynck, 1974, 1987; Pr at & Boulvain, 1982; Pr at *et al.* 1984; Boulvain & Pr at, 1986; Coen-Aubert, Pr at & Tourneur, 1986; Pr at, Ceuleneer & Boulvain, 1987; Bultynck *et al.* 1991; Casier & Pr at, 1991, 2013; Coen-Aubert, 1992, 2000, 2002; Pr at & Kasimi, 1995; Bultynck & Dejonghe, 2001; Gouwy & Bultynck, 2003; G. Poulain, unpub. Masters thesis, Univ. Liège, 2006; Boulvain *et al.* 2009; Maillet, Milhau & Dojen, 2013). The Belgian Givetian carbonate platform shows important N–S and E–W facies variations (Bultynck & De-

jonghe, 2001; Boulvain *et al.* 2009). As a result of the remarkable outcrop conditions, the southern and northeastern portions of the Dinant Syncline have been the focus of most of the investigations cited above whereas its northwestern area has suffered a lack of interest. Consequently, the reconstruction of lateral and vertical facies belt development within this platform has remained incomplete and hampers further palaeogeographic and palaeoenvironmental interpretation.

Over the last decade, magnetic susceptibility (MS) has been used extensively as a palaeoenvironmental, palaeoclimatic proxy and as a correlation tool (B abek *et al.* 2010; Boulvain *et al.* 2010; Michel *et al.* 2010; Whalen & Day, 2010; Da Silva & Boulvain, 2012), and an extended database of MS measurements is available for numerous Devonian sections in Belgium (Da Silva *et al.* 2013; Pas *et al.* 2015) and worldwide (Hladil *et al.* 2006; Whalen & Day, 2008; Kopt ikov a *et al.* 2010; Kopt ikov a, 2011; Pas *et al.* 2014). Moreover, a recent IGCP project (IGCP-580, UNESCO funding) has focused on the application of MS as a palaeoclimatic proxy, specifically for the Devonian. This has

†Author for correspondence: dpas@ulg.ac.be

allowed a better understanding of the use of MS techniques as a tool for high-resolution correlation and palaeoenvironmental reconstructions (e.g. IGCP 580 project; Da Silva *et al.* 2014). However, MS measurements need to be combined with the outcomes of other techniques such as geochemical data (Riquier *et al.* 2010; Da Silva *et al.* 2013), magnetic properties analyses (Devleeschouwer *et al.* 2010; Da Silva *et al.* 2012), sedimentology (Mabille *et al.* 2008b; Da Silva *et al.* 2009), biostratigraphy, etc. to provide robust insights on the applicability of this proxy as a correlation tool or as a palaeoclimatological indicator. Indeed, it is essential to decipher whether the recorded MS signal represents a primary depositional-induced imprint (e.g. change in detrital supply basinwards, leading to a link between MS and independent geochemical proxies related to detrital inputs such as Zr, Al, Rb, etc.) or a post-depositional secondary signature (e.g. diagenesis and metamorphism).

This paper focuses on the La Thure section, from the northwestern margin of the Dinant Syncline. This section is worthy of interest for the following reasons: (1) it is an outstanding outcrop in an area where outcrops are rare and (2) it provides a relatively continuous record of a several million-year-long stratigraphic interval. This paper proposes detailed sedimentological analyses and illustrates the fascinating facies diversity that shaped the early–late Givetian platform on the northwestern margin of the Dinant Syncline. Thorough comparison with the southern extension of this platform was done in order to improve the knowledge on the distribution of the main facies belts and their evolution over million-year scales within the Dinant Basin. Moreover, we have set up a large set of MS and geochemical data in order to clearly constrain the link between MS and siliciclastic input proxies for each section, and to build a robust high-resolution MS reference profile for the shallow water of the early to late Givetian platform in Belgium. The MS million-year trends that are recorded in this profile will allow us to further test the applicability of MS as a correlation tool within the Rhenohercynian Basin, but also with other basins. The geochemical dataset is also used to gain a better comprehension of the palaeoredox and facies change history within the Dinant Basin. Moreover, this large set of data (including MS and geochemistry) will also serve to increase knowledge on the applicability and limitation of MS as a tool for palaeoenvironmental reconstruction.

2. Geological context

During Middle Devonian time, Belgium was situated around 20° S (Torsvik *et al.* 2012) along Laurussia's southeastern margin (Fig. 1a). During Givetian time, this area was part of a wide carbonate platform along the northern passive margin of the Rhenohercynian Ocean. In terms of modern geography, the Givetian carbonate platform extends from the Avesnois Basin (northern France) to Aachen (western Germany) in the

east. In addition, isolated carbonate complexes grew in the east and the southwest, i.e. the Rhenish Massif (Rheinisches Schiefergebirge, e.g. Brilon Reef Complex; Pas *et al.* 2013) and Torbay Reef Complex of SW England, respectively (Torbay Reef Complex; Garland, Tucker & Scrutton, 1996). In Belgium, Givetian sediments crop out all along the border of the Dinant and Vesdre synclines, in the Philippeville Anticline and along the southern border of the Brabant Massif, within the Brabant Para-autochthonous region and the Haine–Sambre–Meuse Overturned Thrust sheets (for precise location see Belanger *et al.* 2012, fig. 5), which are all large-scale units of the Rhenohercynian fold-and-thrust belt (Fig. 1b). This extensive tectonic structure was formed during Carboniferous to Permian time as a consequence of the collision between the Laurussia and Gondwana supercontinents during the Variscan orogeny. Several authors (e.g. Molina Garza & Zijderveld, 1996; Zwing *et al.* 2005; Da Silva *et al.* 2012) highlighted that during this orogeny, the rocks belonging to the Rhenohercynian fold-and-thrust belt were affected by remagnetization.

The La Thure section is located in southwestern Belgium (50° 17' 11" N, 4° 09' 40" E) and belongs to the northwestern border of the Dinant Syncline (Fig. 1b). The section covers sediments ranging from the Givetian to the lower Frasnian. Recently, the Frasnian part of the La Thure section has been the topic of a multidisciplinary study (sedimentology, geochemistry and MS) published by Pas *et al.* (2015).

The Givetian lithostratigraphic units, according to the Belgian Givetian lithostratigraphic chart defined in Bultynck & Dejonghe (2001), were established for the southern border of the Dinant Syncline. They are associated with conodont zones (Bultynck, 1974, 1987; Gouwy & Bultynck, 2003) and with the main transgression–regression cycles (Johnson, Klapper & Sandberg, 1985) (Fig. 1c). Five formations lying in the Givetian crop out on the southern border of the Dinant Syncline. From base to top those formations are, respectively (Fig. 1c, d): (1) the upper part of the Hanonet; (2) Trois-Fontaines; (3) Terres d'Hairs; (4) Mont d'Hairs and (5) Fromelennes formations. Lateral equivalents of these five formations on the northern border of the Dinant Syncline are the Nèvremont and Le Roux formations (Fig. 1d). In the La Thure section, the upper part of the Terre d'Hairs Fm and the Mont d'Hairs and Fromelennes formations are observed (see also local geological map of Hennebert, 2008), and their lithologies remain relatively similar compared to the Dinant Syncline southern border. However, the Mont d'Hairs and Fromelennes formations show a reduced thickness, respectively, of ~50 % and ~25 % (in comparison with the formations as defined in the type area). Considering the similar lithologies, we assume that the Givetian conodont biostratigraphy developed for the southern border of the Dinant Syncline (Bultynck, 1974, 1987; Gouwy & Bultynck, 2003; Narkiewicz, Narkiewicz & Bultynck, 2015) can convey an idea of the extension of the conodont zones. According to this, the

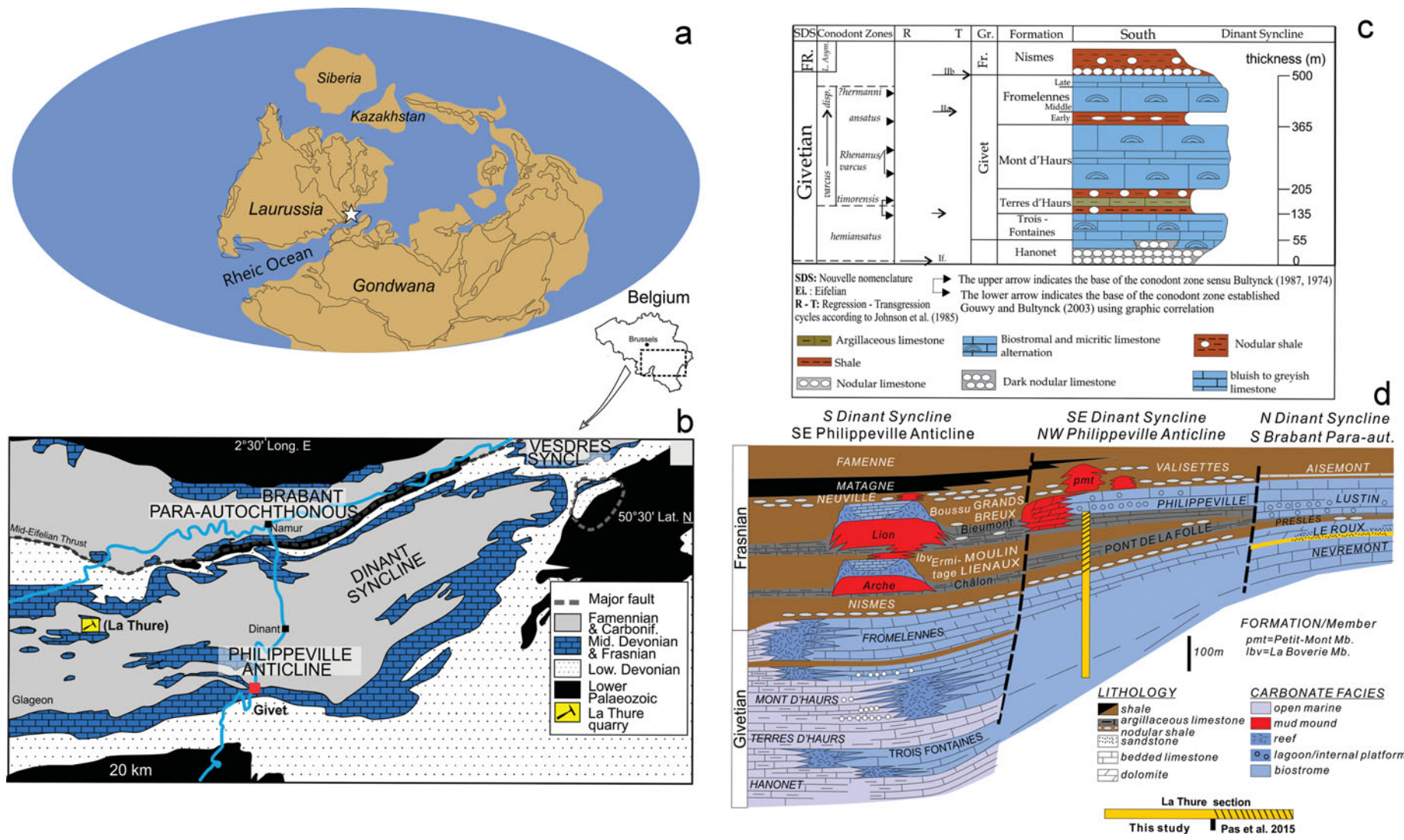


Figure 1. (Colour online) (a) Location of Belgium on the eastern margin of Laurussia during Devonian time (simplified from Kiessling, Flügel & Golonka, 2003). (b) Simplified geological map of southern Belgium with location of La Thure (NW of the Dinant Syncline) and Givet (south of the Dinant Syncline). For the location of the Haine–Sambre–Meuse Overturned Thrust sheets refer to the map of Belanger *et al.* (2012) (c) Givetian lithostratigraphic column established for the southern border of the Dinant Syncline showing conodont zones (Bultynck, 1974, 1987; Gouwy & Bultynck, 2003) and the main transgressive–regressive cycles (Johnson, Klapper & Sandberg, 1985). (d) Integrated lithostratigraphical and palaeogeographical framework for the Givetian and Frasnian of Belgium. Relative positions of the reefs show the retrogradation–progradation patterns of the carbonate platforms (modified after Boulvain *et al.* 2009).

Givetian strata in the La Thure section likely covers an interval extending from the early Givetian *Polygnathus timorensis* Zone to the late Givetian Lower *Mesotaxis falsiovalis* Zone.

Based on Givetian sections from the Avesnes (northern France), Dinant and Namur basins, which belong to the Dinant Syncline, Haine–Sambre–Meuse Overturned Thrust sheets and Brabant Para-autochthonous region, Pr at & Mamet (1989) defined 13 microfacies covering a large range of environments extending from open-marine and under the wave action zone, to reefal complexes, lagoons and evaporitic sabkhas including laminites and palaeosols. According to these authors, the Belgian Givetian carbonate platform was composed of several kilometre-sized faulted blocks. Furthermore, as summarized by Boulvain *et al.* (2009), the Givetian deposits in Belgium can be divided into three ENE–WSW-directed facies belts (Fig. 1d): (1) the most distal part of the platform (‘southern belt’) located along the southern margin of the Dinant Syncline is characterized by ramp and off-reef to internal platform deposits; (2) the ‘central belt’ cropping out in the Philippeville Anticlinorium and southeast of the Dinant Syncline, which is poorly known, and (3) a ‘northern belt’, in the north of the Dinant Syncline and in the south of the Brabant Para-autochthonous region, characterized mainly by the shallowest marine deposits and alluvial deposits. The shallowest to deepest depositional environments of the Givetian platform are in accordance with the general northerly transgressive sea-level trajectory, which progressively submerged the Old Red Continent from Emsian to late Frasnian time (Pr at & Bultynck, 2006).

3. Methods

A detailed bed by bed description and sampling of the La Thure section (Fig. 2; 153 m in thickness) was performed with a sampling interval of 25 to 45 cm, depending on the outcrop condition. MS measurements were undertaken on all the collected samples (~400 samples). Each sample was measured three times with a KLY-3 (Kappabridge from AGICO) and weighted with a precision of 0.01 g. This allows the definition of the low-field mass-calibrated MS for each sample and the establishment of the MS curve (Fig. 10a). For microfacies analysis we selected around 200 samples for thin-section preparation (thin-sections are stored at the sedimentary petrology laboratory of the University of Li ge, samples TUR 100–TUR 311). The textural classification used to characterize the microfacies follows Dunham (1962) and Embry & Klovan (1972). Estimation of sorting is based on the visual charts of Pettijohn, Potter & Siever (1972) and visual percentage estimations are based on Baccelle & Bosellini (1965). Thin-sections were stained using Dickson solution to differentiate calcite, dolomite, ferroan calcite and ferroan dolomite (Dickson, 1965). A group of 30 samples (~1 sample per 5 m) was analysed for major- and trace-element concentrations at Activation

Laboratories Ltd (Ancaster, Ontario, Canada). Analyses were performed by inductively coupled plasma mass spectrometry (ICP-MS) (major, minor and trace elements). The samples were prepared by fusion with sodium peroxide, Na₂O₂, which totally solubilizes all the minerals analysed in an aqueous solution after treatment.

4. Results

4.a. Description of the La Thure section (Fig. 2)

The measured Givetian section in the La Thure quarry is ~153 m thick with strata oriented N90° E and dipping 70° S. According to the Belgian Givetian lithostratigraphic charts defined by Pr at & Bultynck (2006) and data from the geological map of Hennebert (2008), the Terres d’HOURS, Mont d’HOURS and Fromelennes formations can be identified. In the La Thure section, only the upper part of the Terre d’HOURS Fm is observed. It is followed by the Mont d’HOURS and Fromelennes formations. These last two formations show reduced thicknesses, respectively, of ~50 % and ~25 % in comparison with that observed in the type areas, as presented in Figure 1c.

The Terres d’HOURS Fm (~8 m thick; Figs 1, 2) corresponds mainly to centimetre- to decimetre-thick dark-grey highly argillaceous limestone beds intercalated with decimetre-thick limestone locally rich in crinoid debris. This formation lies within the *timorensis* Zone.

The Mont d’HOURS Fm (~56 m thick; Figs 1, 2) is mainly composed of several decimetre-thick, well-bedded black to dark-grey limestones. Conspicuous within the lower and middle part are abundant gastropod shells (scattered within the sediment or organized into packed decimetre-thick levels parallel to the bedding; Fig. 2a). Other observed fossils include tabulate corals, stromatoporoids, crinoids and brachiopods. Locally, a well-developed bioturbated fabric can be observed (Fig. 2b). This formation lies within the *rhenanus* (Lower *P. varcus*) Zone.

The Fromelennes Fm (~85 m thick; Figs 1, 2) can be divided into three lithological units (U1–U3). Unit 1 (U1; from 64 to 93 m) is characterized by grey decimetre- to metre-thick beds. The proportion of gastropods is low and the abundance of reef-builder debris such as tabulate and rugose corals, and lamellar, branching and bulbous stromatoporoids is significant. Crinoids and brachiopods are also a major component of the faunal assemblage. The topmost part of Unit 1 is characterized by two metre-thick limestone beds showing abundant and large debris of reef-building organisms. Locally, stromatoporoids reach more than 50 cm in size. Unit 2 (U2; from 93 to 150 m) is mainly composed of decimetre-sized light-grey to ocherous limestone beds (corresponding to dolomitized beds). The conspicuous characteristic of this U2 is the abundance of a thin millimetre- to centimetre-sized laminar fabric (Fig. 2c). The fauna is usually poorly rep-



Figure 2. (Colour online) Top: view of the Givetian section in the La Thure quarry with the three investigated formations and the location of photographs. (a–e) Close up of different facies, the black arrows point to the stratigraphic base. THR – Terres d’Hauris Fm. (a) Gastropod-rich levels in the lower portion of the Mont d’Hauris Formation. (b) Laminated limestone, showing vertical burrows filled by calcite exposed within the lower portion of Unit 1, Mont d’Hauris Fm. (c) Slightly yellowish laminated limestone commonly occurring within Unit 2, Fromelennes Fm. (d) Decimetre-thick level (delimited by dashed lines) enriched in branching stromatoporoids (note that the lower boundary of this level is characterized by an erosion surface while the upper boundary is overlain by a thin laminated fabric) – erratic block near upper portion of the section corresponding to the Fromelennes Fm. (e) Intraformational breccia overlying a level of laminated limestone.

resented throughout the unit, whereas within the upper part, centimetre- to decimetre-thick, well-sorted laminated levels enriched in branching stromatoporoids such as *Stachyodes* and *Amphipora* occur (Fig. 2d). These levels are usually overlying laminated limestone or dolostone with a sharp erosive lower boundary. Locally, a well-preserved intraformational breccia developed from the laminated limestone can be observed (Fig. 1e). This formation covers a stratigraphic interval ranging from the *ansatus* to Lower *falsiovalis* zones.

Throughout Unit 2, organisms are essentially debris of reef-builders, such as branching and bulbous stromatoporoids and branching tabulate corals. The overlying Unit 3 (U3; from 150 to 153 m) is mainly characterized by decimetre- to several decimetre-thick dark-grey to dark-blue beds locally showing abundant brachiopod shells and crinoids. Unit 3 is overlain by ocherous limestone interlayered with black carbonaceous limestone belonging to the Nismes Fm of Frasnian age (for a detailed description see Pas *et al.* 2015).

4.b. Microfacies descriptions of the La Thure section (Table 1; Figs 3–8)

The lower–upper Givetian sequence in the La Thure section represents an outstanding example of the extensive diversity occurring in the Middle Devonian reefal realm. The description of texture, faunal and floral assemblages, preservation and sorting of organisms in combination with selected literature (Neumann, Pozaryska & Vachard, 1975; Strasser, 1986; Pr eat, Ceuleneer & Boulvain, 1987; Skompski & Szulczewski, 1994) allowed us to define 18 microfacies, which are summarized in Table 1 and described below. Texture reflects the level of water agitation during deposition, while the biotic composition is a consequence of more complex parameters such as the oxygen level, the water depth, the level of restriction from the open sea, the hydrodynamic conditions, etc. Our microfacies classification follows approximately the distal to proximal depositional setting (considering that some microfacies could be laterally equivalent). Furthermore, some microfacies represent event-like features, and are thus not limited to one or another depositional setting. For example, limestone with a concentration of shell material can be formed in different shallow-marine and deep-marine facies zones (e.g. Fl ugel, 2004, p. 799). Therefore, our classification of microfacies in a distal–proximal transect considers (1) the stratigraphic position, (2) the lateral extension and (3) the taphonomy of fossils that characterize the shell beds within the sedimentary sequence (e.g. Kidwell & Bosence, 1991; F ursich & Oschmann, 1993). The obtained microfacies curves demonstrate a complex evolution of carbonate platform types throughout the early–late Givetian interval. Starting with a homoclinal ramp profile the carbonate platform evolves through a discontinuously rimmed shelf to a drowning shelf in latest Givetian time. Interpreted microfacies are thus considered to belong to a wide spectrum of carbonate platform profiles with

two end-members. The subdivisions between carbonate platform types and related interpretations are discussed in Section 5. The system used to denote the facies underlines both the model type (DS – drowning shelf, RS – rimmed shelf and RP – ramp) and the studied locality (LT – La Thure).

4.b.1. Drowning shelf: DS microfacies

DS-LT1: mudstone and wackestone with densely packed brachiopod–bivalve shell levels (Fig. 3)

This microfacies exclusively occurs within Unit 3 of the Fromelennes Fm. It is mainly characterized by mudstone and wackestone textures, but, locally, densely packed centimetre-thick brachiopod–bivalve shell packstone and rudstone levels occur. The transition from mudstone–wackestone to these packed levels is gradual (erosional surfaces are not observed). Packed levels correspond to centimetre-sized accumulations of brachiopod (dominant), bivalve and gastropod shells embedded in a micritic matrix and show clear bioturbated fabrics. The shells of the brachiopods are relatively well preserved (locally articulated shells occur) and show sizes varying from 0.3 to 2.5 cm with an average of around 0.6 cm. Large bivalve shells are commonly broken but juveniles are better preserved. Sorting is poor to moderate and bioturbation commonly affects the sediment; this is underlined by the reorganization of shells ('nesting'). Other fossils include common crinoid ossicles and plates, rare *umbrella* (i.e. charophycean algae, Mamet, 1970), solitary rugose corals, ostracods, stromatoporoid debris and unidentified bioclasts. Crinoids are relatively well preserved and often millimetre in size. The matrix is a fine-grained micrite, locally dolomitized.

Interpretation

Brachiopod and bivalve shells embedded in a micritic matrix and the common occurrence of crinoids point to an open-marine setting with relatively quiet conditions prior to deposition. The poor to moderate sorting of shells and the vertical bioturbation corroborate this interpretation. According to F ursich & Pandey (1999) the significant density of shells may be the result of several processes: a high productivity combined with low sedimentary rate and occasional winnowing. According to Mamet (1970) the occurrence of *umbrella* indicates a nearshore setting and abnormal levels of salinity (high or poor) while echinoderms and brachiopods are in favour of open-marine conditions. Considering the thick inter- to supratidal lagoonal sequence developed beneath (e.g. Unit 2), deposition of DS-LT1 could have occurred within a proximal shelf setting concurrently with the re-establishment of open-marine conditions. This hypothesis is also confirmed by the overlying open-marine Frasnian shale sequence (Pas *et al.* 2015). The occurrence of bioclasts from various environments might be the result of distal tempestites. However, the high-rate of bioturbation that affected the sediment after deposition destroyed original

Table 1. Synthesis of microfacies for the Givetian in the La Thure section (western Belgium)

Microfacies number	Name	Main diagnostic features	Bedding, colour and sedimentary structures	Depositional setting
<i>Drowning shelf model (DS)</i>				
DS-LT1	Brachiopod–bivalve shell packstone–rudstone	Limestone with brachiopods, bivalves, gastropods, crinoids. Poorly to moderately sorted. Common bioturbations	Decimetre-thick homogeneous dark-grey to black limestone beds	Drowning shelf below the FWFB
<i>Ramp model (RP)</i>				
RP-LT1	Bioclastic lime mudstone to packstone	Limestone rich in insoluble residues commonly dolomitized. With poorly preserved crinoids, brachiopods and unidentified shells, gastropods, ostracods, bryozoans, worm tubes, tabulate corals and stromatoporoids	Centimetre- to decimetre-thick black to dark-grey argillaceous beds	Mid- to distal-ramp below the FWFB with storm deposit occurrences
RP-LT2	Crinoidal packstone–grainstone	Coarse-grained crinoids (with micritized rims), gastropods (with common micrite filling internal moulds) and bioturbations	Centimetre- to decimetre-thick argillaceous black to dark-grey limestone beds	Mid- to distal-ramp below the FWFB with storm deposit occurrences
<i>Rimmed shelf model (RS)</i>				
Facies belt 1: Biostrome and fore-reef shelf				
RS1-LT1	Open-marine bioclastic wackestone and packstone	Crinoids, brachiopods, ostracods, trilobites, bryozoans, tentaculitids and local debris of branching tabulate and rugose corals, and stromatoporoids	Decimetre-thick coarse-grained dark-blue limestone beds	Open-marine setting located below the FWFB slightly influenced by reefal construction (barrier-reef or patch-reef)
RS1-LT2	Coral–stromatoporoid rudstone/floatstone	Decimetre-sized stromatoporoids (laminar and bulbous), solitary rugose corals, branching tabulate corals, crinoids, brachiopods, trilobites	Coarse-grained dark-blue to dark-grey limestone with large and broken reef-builders in non-living position	Open-marine setting located below the FWFB strongly influenced by reefal construction (barrier-reef or patch-reef)
Facies belt 2: Bioclastic shoals				
RS2-LT3	Calcmicrobial bio-lithoclastic grainstone	<i>Girvanella</i> , <i>Sphaerocodium</i> , gastropods, rare and poorly preserved brachiopods, worm tubes, stromatoporoids	Decimetre-thick dark-blue to dark-grey limestone beds	Open-marine temporarily agitated setting located on the internal shelf margin
RS2-LT4	Peloidal–lithoclastic grainstone with gastropods and mud-coated grains	Peloids and micritic lithoclasts, gastropods, brachiopods, crinoids, ostracods and rare tabulate corals and bryozoans	Decimetre-thick dark-blue to dark-grey limestone	Peloid bars within the FWFB at the internal shelf margin

Table 1. Continued

Microfacies number	Name	Main diagnostic features	Bedding, colour and sedimentary structures	Depositional setting
Facies belt 3: Internal shelf with good circulation				
RS3-LT5	Mudstone to packstone with lithoclastic – brachiopod rudstone–grainstone layers/pockets	Brachiopod shells, thick-walled ostracods, gastropods, worm tubes and micritic lithoclasts within grainstone	Decimetre-thick dark-blue limestone	Internal shelf with open-water circulation located under the FWWB but likely subject to tides or storm flow
RS3-LT6	<i>Magnella</i> shell grainstone and rudstone	<i>Magnella</i> shells and peloids	Pluri-centimetre-thick beds	Storm deposits within an internal shelf setting
RS3-LT7	Stromatoporoid rudstone	Broken bulbous and dendroid stromatoporoids, branching tabulate, fasciculate rugose corals, <i>Sphaerocodium</i> and frequent Paleosiphonocladales	Decimetre-thick dark-blue beds	Setting with limited connection to fully marine setting
RS3-LT8	Issinellids–palaeoberesellids wackestone–packstone	Abundance of issinellid and palaeoberesellid algae, brachiopod shells, ostracods and <i>Girvanella</i> oncoids	Decimetre-thick dark-blue beds	Subtidal setting in the vicinity of Paleosiphonocladales
RS3-LT9	Burrowed calcisphere mudstone	Vertical burrow filled by calcite	Decimetre-thick dark-blue beds	Protected setting below the FWWB
RS3-LT10a	Oolitic grainstone–packstone	Type 3 ooids and locally Type 1 of Strasser (1986)	Centimetre- to decimetre-sized light- to dark-grey bed	Oolitic shoal developed in intermittently agitated water in internal shallow platform setting
Facies belt 4: Internal restricted shelf				
RS4-LT10b	Oolitic peloidal grainstone–packstone	Type 2 and 4 ooids of Strasser (1986)	Centimetre- to decimetre-sized light- to dark-grey bed	Lagoonal setting with calm- to moderately agitated water energy
RS4-LT10c	Oolitic lithoclastic grainstone–packstone	Type 4 ooids of Strasser (1986)	Centimetre- to decimetre-sized light- to dark-grey bed	Lagoonal setting with local higher energy-event
RS4-LT11	Lithoclastic rudstone	Peloidal and oolitic grainstone lithoclasts	Centimetre- to decimetre-sized light- to dark-grey bed	Lagoonal setting in the vicinity of RS3-LT10a
Facies belt 5: Evaporitic internal shelf				
RS5-LT12	Dendroid stromatoporoid rudstone–floatstone	<i>Stachyodes</i> and <i>Amphipora</i> , <i>Girvanella</i> , <i>Renalcis</i> lumps and stromatoporoids	Pluri-decimetre-sized beds with local erosive base	Reworked stromatoporoid patch-reef in internal setting
RS5-LT13	Algal microbial boundstone	Micritic tubular structures, clotted fabric, ostracods and worm tubes	Centimetre- to decimetre-sized beds	Shrub-like structure in quiet shallow-marine internal setting
RS5-LT14	Laminated mudstone – peloidal grainstone–packstone	Alternation of peloidal grainstone and mudstone layer or light and darker micritic laminae with locally well-spread silt-sized quartz	Decimetre-thick beds	Tidal-channel and levees bordering channel and intertidal ponds in supratidal setting
RS5-LT15	Intraclastic rudstone–grainstone	Centimetre-sized mudstone and grainstone intraclasts, oolite and sparitic cement	Decimetre-thick ocherous beds	Reworking in tidal-channel setting

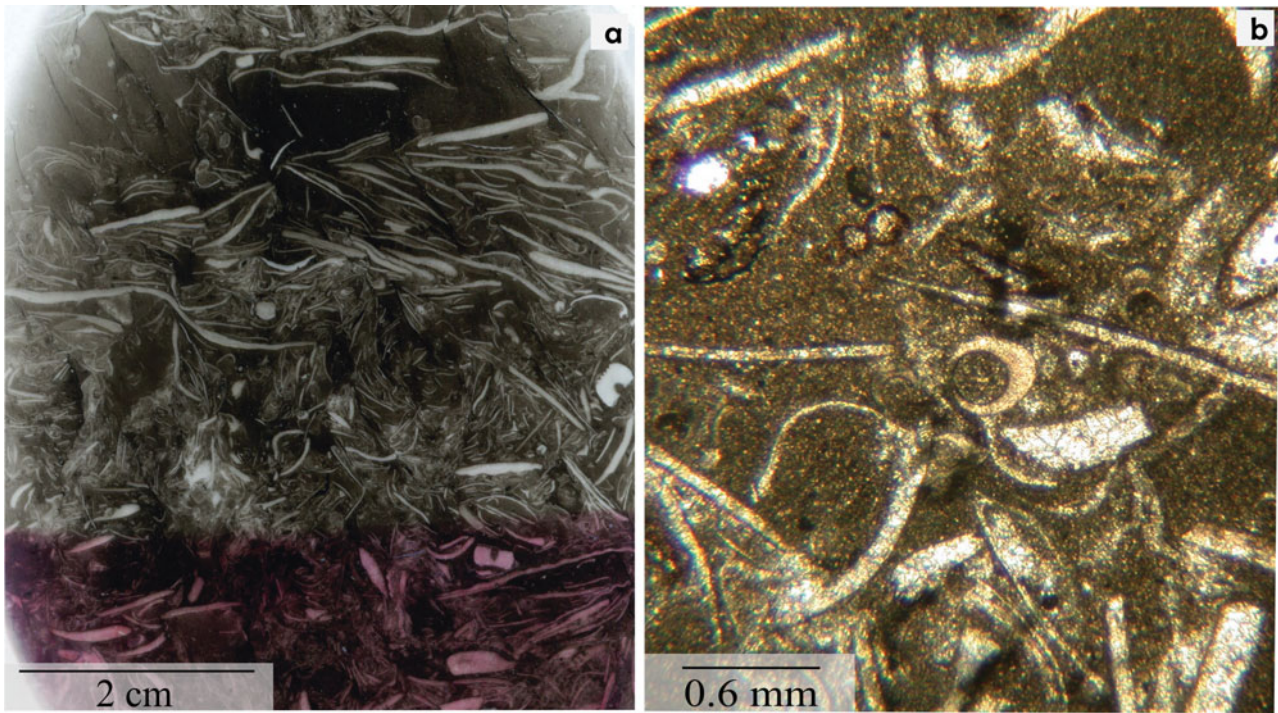


Figure 3. (Colour online) Microfacies DS-LT1 – drowning shelf – from the Givetian of the La Thure section, Belgium. Photomicrographs of thin-sections are oriented perpendicular to the bedding. Numbers preceded by ‘TUR’ correspond to bed numbers. (a) Shell packstone and rudstone (TUR 310, scanned thin-section, with alizarine staining). (b) Shell packstone including *umbrella* (centre of the photograph).

fabrics and hampers testing of this hypothesis. In conclusion, this microfacies could correspond to an accumulation of shells in a calm open-marine setting, subjected to storm-related winnowing and bioturbation, probably during a time of transgression (e.g. end Givetian transgressive pulse).

4.b.2. Ramp: RP microfacies

RP-LT1: bioclastic lime mudstone to packstone

This microfacies only occurs at the base of the studied section attributed to the Terre d’Hairs Fm. It is characterized by a commonly dolomitized, fine-grained matrix, an open-marine faunal assemblage and the occurrence of millimetre- to centimetre-thick layers rich in poorly preserved crinoids and finely broken skeletal debris (Fig. 4a). Fossils are poorly to moderately preserved, except for some larger tabulate corals and stromatoporoids. The main fauna is represented by brachiopods (locally complete centimetre-sized shells) and other unidentified shells (often finely broken and strongly recrystallized) and crinoid debris (from 0.4 to 2 mm). Less common organisms are gastropods, ostracods, branching bryozoans, worm tubes and rare tabulate corals and stromatoporoids. Locally, the sediment is significantly bioturbated and shows clear examples of circular burrows filled by peloidal grainstone (Fig. 4b). In other cases, bioturbation is recognized by the reorganization of bioclasts. Rarely, brachiopod shells show infra-millimetre-thick encrustation by porostromates. Finely broken unidentifiable shells are locally the main

constituents of sediment corresponding to shell hash. Crinoidal-rich layers, associated with fine-grained brachiopod and ostracod shells, show a packstone texture and the transition from lime mudstone–wackestone in those layers is gradual. Insoluble residues are commonly observed between the fine-grained bioclasts.

Interpretation

Crinoids, brachiopods and bryozoans indicate a depositional environment below the fair weather wave base (FWWB) within open-marine conditions. The common occurrence of gastropods implies a shallow-marine environment while moderate to poorly preserved levels of bioclasts indicate that organisms were subjected to relatively long exposure on the sea-floor prior to burial. The occurrence of millimetre- to centimetre-thick layers mainly characterized by crinoid debris accumulations indicates high-energy events such as tempestites that triggered transport and concentration of debris basinwards. The dominance of crinoid debris in those layers also suggests the occurrence of a crinoidal meadow in a shallower location. The lack of clues from microfacies RP-LT1 makes it difficult to determine whether this microfacies represents a homoclinal ramp or an external shelf reef. Occurrences of this microfacies within lithologies belonging to the Terre d’Hairs Fm, which are commonly interpreted as ramp-related in southern Belgium (Mabille *et al.* 2008a; Boulvain *et al.* 2009), suggest deposition on a ramp profile. In conclusion, the depositional setting might correspond to a mid- to distal-ramp located below the FWWB and locally influenced by higher energy events such as storms

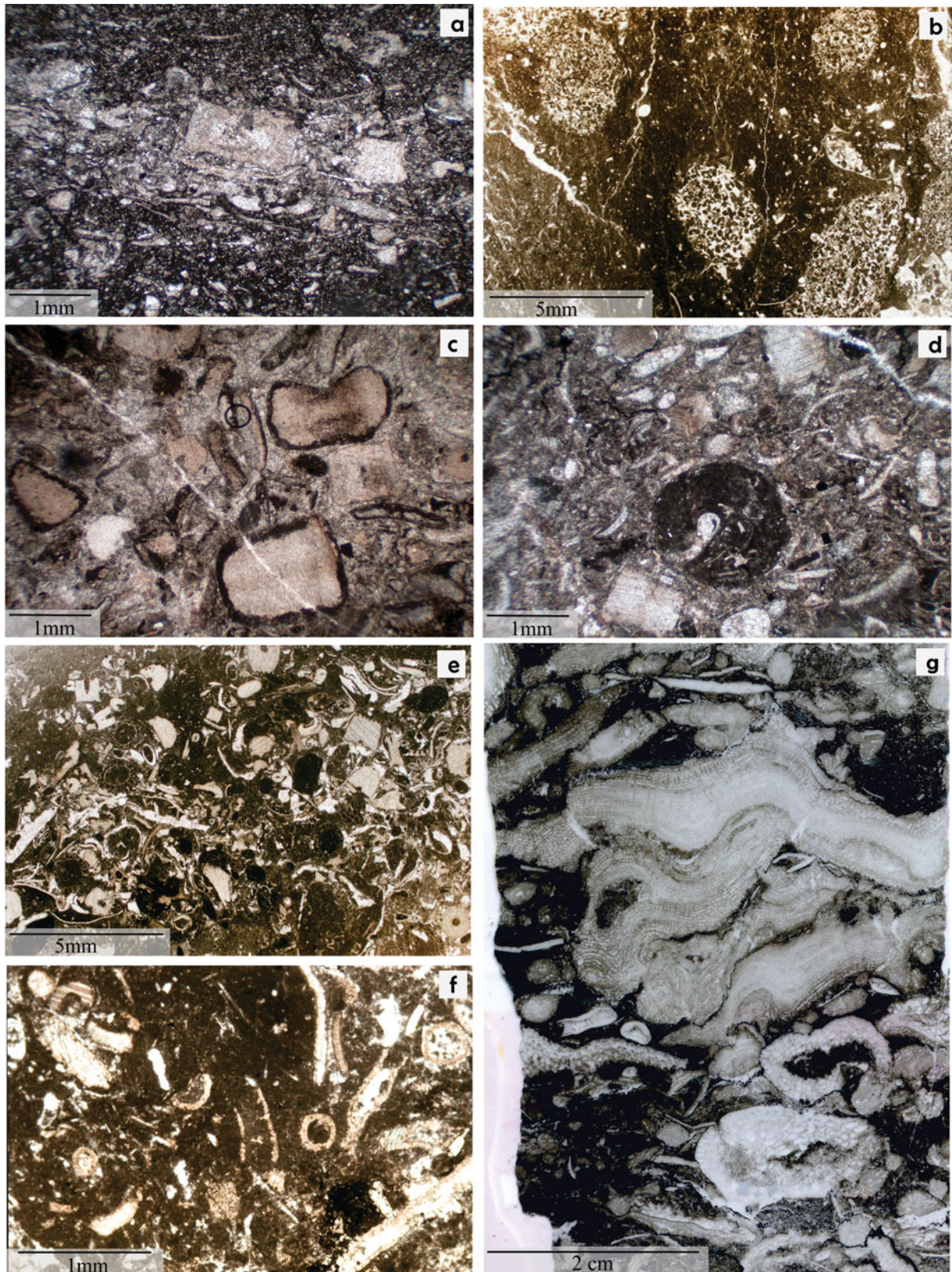


Figure 4. (Colour online) Microfacies RP-LT1–2 and RS1-LT1–2 from the Givetian of the La Thure section, Belgium. Photomicrographs of thin-sections are oriented perpendicular to the bedding. Numbers preceded by ‘TUR’ correspond to bed numbers. (a) RP-LT1 mid- to distal-ramp setting: crinoidal packstone rich layer within a dolomitized mudstone and wackestone (TUR 100b, transmitted light). (b) RP-LT1 mid- to distal-ramp setting: bioclastic mudstone–wackestone showing peloidal grainstone filling burrows (TUR 108, transmitted light). (c) RP-LT2 mid- to distal-ramp setting: coarse-grained grainstone, with crinoids showing micritized rim (TUR 100, transmitted light). (d) RP-LT2 mid- to distal-ramp setting: crinoidal packstone showing gastropod internal moulds filled by micrite (TUR 100, transmitted light). (e) RS1-LT1 biostrome and fore-reef shelf: bryozoan crinoidal packstone (TUR 181c, transmitted light). (f) RS-LT1 external reef and fore-reef shelf: bioclastic packstone showing remains of issinellid algae (TUR 195, transmitted light). (g) RS1-LT2 biostrome and fore-reef shelf: lamellar stromatoporoid rudstone (TUR 202, scanned thin-section).

that triggered the transport of these bioclasts towards deeper marine areas.

RP-LT2: crinoidal packstone–grainstone (Fig. 4c)

This microfacies only occurs in a few decimetre-thick beds located at the base of the studied section attributed to the Terre d’Hauris Fm and is intercalated within microfacies RP-LT1. This microfacies is commonly dolomitized but the texture and faunal assemblage are preserved locally. When dolomitization does not affect the main characteristics of this microfacies, an abundance of crinoid ossicles and plates showing a micritized rim (Fig. 4c) is typical. Crinoids range from 0.5 to 2 mm with an average size of around 1 mm. Other fossils are generally broken and represented by gastropods, brachiopods, ostracods, rare bryozoans and finely comminuted unidentifiable debris. Gastropods commonly display an internal mould filled by micritic matrix (Fig. 4d). Burrows occur and are underlined by a core filled with finely broken organisms in a micritic matrix.

Interpretation

The abundance of crinoids and the occurrence of brachiopods and bryozoans within limestone with a packstone–grainstone texture suggest an open-marine environment likely close to crinoidal meadows and above the FWFB. Crinoid debris and gastropods packed in centimetre-thick levels surrounded by microfacies RP-LT1 suggest a deposition related to high-energy events, and in the vicinity of the setting assumed for RP-LT1. Indeed, RP-LT2 is surrounded by microfacies RP-LT1, and RP-LT1 is interpreted as having been deposited in an open-marine mid- to distal-ramp setting below the FWFB.

4.b.3 Rimmed shelf: RS microfacies

The complexity and diversity of depositional settings occurring in this carbonate rimmed shelf profile leads to its subdivision into five facies belts (RS1–RS5): (RS1) biostrome and fore-reef shelf; (RS2) bioclastic shoals; (RS3) internal shelf with fair circulation; (RS4) internal restricted shelf; (RS5) internal evaporitic shelf.

Facies belt 1: biostrome and fore-reef shelf

RS1-LT1: open-marine bioclastic wackestone and packstone (Fig. 4e, f)

This microfacies is characterized by open-marine faunal assemblages, embedded in a micritic matrix, showing poor to moderate sorting. Fossils are mostly broken and are represented in decreasing order of abundance by crinoids, brachiopods, ostracods (thick and thin-shelled), bivalves, gastropods, branching and fenestellid bryozoans, trilobites, tentaculitids, Paleosiphonocladales (e.g. issinellids; Fig. 4f) and abundant unidentifiable shells. Locally, debris of branching tabulate corals, rugose corals and poorly preserved branching stromatoporoids occur. From time to time, bioclasts are crushed and very poorly preserved dis-

playing an average size of 0.2 mm. Bivalve shells locally show an irregular micritic envelope up to 0.5 mm thick. Thin shells represent up to 80% of the biological constituents. Complete brachiopod shells are locally filled by a clotted fabric. Pressure-solution processes forming horse-tails and an iden-supported fabric commonly occur. ‘Iden-supported’ is a fabric where idens (bodies that behave as homogeneous entities under chemical and physical conditions) are densely packed and bound by irregular, anastomosing microstylolites (Logan & Semenuik, 1976) (see also caption of fig. 7.18b, p. 318 in Flügel, 2004). Argillaceous-rich millimetre-thick layers and seams parallel to the bedding also occur from time to time.

Interpretation

The abundance of open-marine biota such as trilobites, tentaculitids, bryozoans and crinoids embedded in poorly to moderately sorted micritic sediment indicates deposition within a relatively quiet open-marine setting, likely below the FWFB. The occurrence of reef-building organisms and shallow-water biota/flora, such as gastropods and Paleosiphonocladales, suggests an influence of a shallow to moderate shelf setting. Furthermore, the occurrence of reef-building organisms is in favour of a setting located in the vicinity of reefal constructions such as patch- or barrier-reefs.

RS1-LT2: coral–stromatoporoid rudstone/floatstone (Fig. 4g)

This microfacies occurs mainly in metre-thick beds in the upper part of the Mont d’Hauris Fm and lowermost part of the Fromelennes Fm. It is characterized by the dominance of several decimetre-scaled laminar and bulbous stromatoporoids, branching tabulate corals, encrusting stromatoporoids and solitary rugose corals. These coral and stromatoporoid skeletons are always reworked and broken. The area between the skeletal debris is filled by small and commonly unidentifiable bioclasts embedded in a dark micritic matrix showing a wackestone to packstone texture and commonly dolomitized. Identified bioclasts are trilobites, brachiopods, gastropods, ostracods and rare Paleosiphonocladales. The sediment filling the space between large organisms contains detrital quartz and is relatively similar to RS1-LT1.

Interpretation

The abundance of various and large-sized (several decimetre-sized) coral–stromatoporoid debris in a rudstone/floatstone texture indicates a depositional setting strongly influenced by shallow-marine reefal constructions and likely adjacent to RS1-LT1. A wackestone–packstone texture and bioclasts characterizing the space between large reef-builders are in favour of an environment located below the FWFB in the vicinity of RS1-LT1. The poor to moderate preservation and sorting of reef-building organisms suggests a reworking likely by wave action and a downward transport by gravity processes such as storm or debris-flows.

*Facies belt 2: bioclastic shoals**RS2-LT3: calcimicrobial bio-lithoclastic grainstone*

This microfacies is characterized by the common occurrence of the calcimicrobe *Girvanella/Sphaerocodium* (Fig. 5a) as encrusters and oncoid/lump builders. The *Girvanella* encrustation mainly occurs on gastropod shells and can reach up to several millimetres in thickness. Oncoids and lumps are also frequent and locally millimetre-scaled. Other skeletons are poorly preserved and consist of gastropods (locally complete), brachiopods, worm tube debris (with encrusting *Sphaerocodium*), rare stromatoporoids and crinoids. Another major characteristic of RS2-LT3 is the common occurrence of sub-angular to rounded, variously sized (0.3 to 2 mm) lithoclasts (Fig. 5b) constituted either of peloidal grainstone (e.g. RS2-LT4) or mudstone-wackestone (e.g. RS3-LT5). Locally, calcimicrobial encrustation surrounds lithoclasts of bio- and lithoclastic packstone.

Interpretation

The common occurrence of the calcimicrobe *Girvanella* as coatings on gastropods and oncoids favours a euphotic internal shelf setting. According to Scholle & Ulmer-Scholle (2003) oncoid-like *Girvanella* can form in a setting episodically subjected to strong wave action. The grainstone texture and the occurrence of lithoclasts concur with this interpretation. The local occurrence of brachiopods and crinoids argues for an open-marine environment. This microfacies is likely formed adjacent to an external shelf subjected to strong wave action. The uncommon occurrence of reef-builders indicates that this depositional setting was little influenced by reefal construction.

RS2-LT4: peloidal-lithoclastic grainstone with gastropods (Fig. 5c, d)

Peloids represent over 80% of the grain assemblage; based on the variable size (from 50 to 200 µm) and shape (from sub-angular to sub-rounded) most of them are considered lithic peloids (variable shape and size ranging between 50 and 150 µm; Flügel, 2004, p. 112). Micritic lithoclasts (e.g. micritic allochems larger than 200 µm) are commonly observed. Common poorly preserved and rounded gastropod debris, brachiopods, crinoids, rare ostracod shells and rare tabulate corals, stromatoporoids and bryozoans are observed. When bioclasts are smaller than 500 µm they show intense micritization. Mud-coated grains are common, and sorting of the sediment is moderate to good within a grainstone texture, although local packstone texture occurs.

Interpretation

The main characteristic of RS2-LT4 is the abundance of lithic peloids and micritic lithoclasts. The origins of such allochems are interpreted as syn-sedimentary and post-sedimentary reworking of carbonate mud and micrite. The origins of the other peloids are varied: faecal, micritized grains, direct algal origin and intraclasts (Tucker, 2001). Based on the locally intense

micritization of the bioclasts, the origin of many of these other peloids could be related to micritization. The common occurrence of gastropods points to an internal shelf environment. The relatively good sorting and grainstone texture without any sedimentary structure may suggest the occurrence of peloid bars near the margin of the internal shelf where agitation is important within the FWB. Mud-coated grains favour this interpretation. Furthermore, the occurrence of tabulate corals and stromatoporoids indicates a reefal influence. The local pelmicritic texture might be related to periods of lower energy allowing micritic mud to settle.

*Facies belt 3: internal shelf with fair circulation**RS3-LT5: mudstone to packstone with lithoclastic-brachiopod-rudstone-grainstone layers*

This mudstone-packstone is characterized by a well-developed stylonodular fabric, which commonly hampers a good observation of the original texture. Locally, a significant proportion of clay particles and insoluble residues occur. Faunal assemblages are dominated by brachiopod shells, gastropods, thick-walled ostracods and worm tubes (Fig. 5e). Irregular fenestrae (Fig. 5f) are a common occurrence in the mudstone texture. Peloidal grainstone (e.g. RS2-LT4) commonly fills the internal moulds of brachiopod shells. Another dominant character of this microfacies is the local occurrence of brachiopod-rich, lithoclastic grainstone-rudstone layers (Fig. 5g). Within these layers both lithoclasts and brachiopod shells are abundant (Fig. 6a). Locally, there are also a few grainstone-rudstone pockets, dominated by lithoclasts. Lithoclasts are essentially micritic, well rounded and infra-millimetre to millimetre-scaled while brachiopods range from 0.3 to 1 cm in size and are locally articulated. Grainstone-rudstone layers and pockets are centimetre-scaled and their boundary with the mudstone-wackestone is not clearly visible owing to pressure-solution processes. Within this microfacies, bioturbation and a local clotted fabric occur. When argillaceous material is abundant, dolomitization is well developed.

Interpretation

The mudstone-wackestone texture and the faunal assemblage and its relatively good preservation indicate a quiet depositional setting for this microfacies, allowing settling of mud and the preservation of organisms as in microfacies RS2-LT3. However, the faunal assemblage implies an internal shelf with a fair circulation. Grainstone-rudstone layers or pockets occurring in this microfacies suggest a temporary storm-induced increase in the water energy level allowing an accumulation of brachiopods and the reworking of micritic clasts in a grainstone-rudstone texture.

RS3-LT6: Magnella shell grainstone and rudstone (Fig. 6b, c)

This microfacies only occurs within three centimetre-sized beds in the lower portion of the Mont d'Hours Fm. These beds are intercalated within RS3-LT5 mudstone-wackestone. The conspicuous characteristic of this mi-

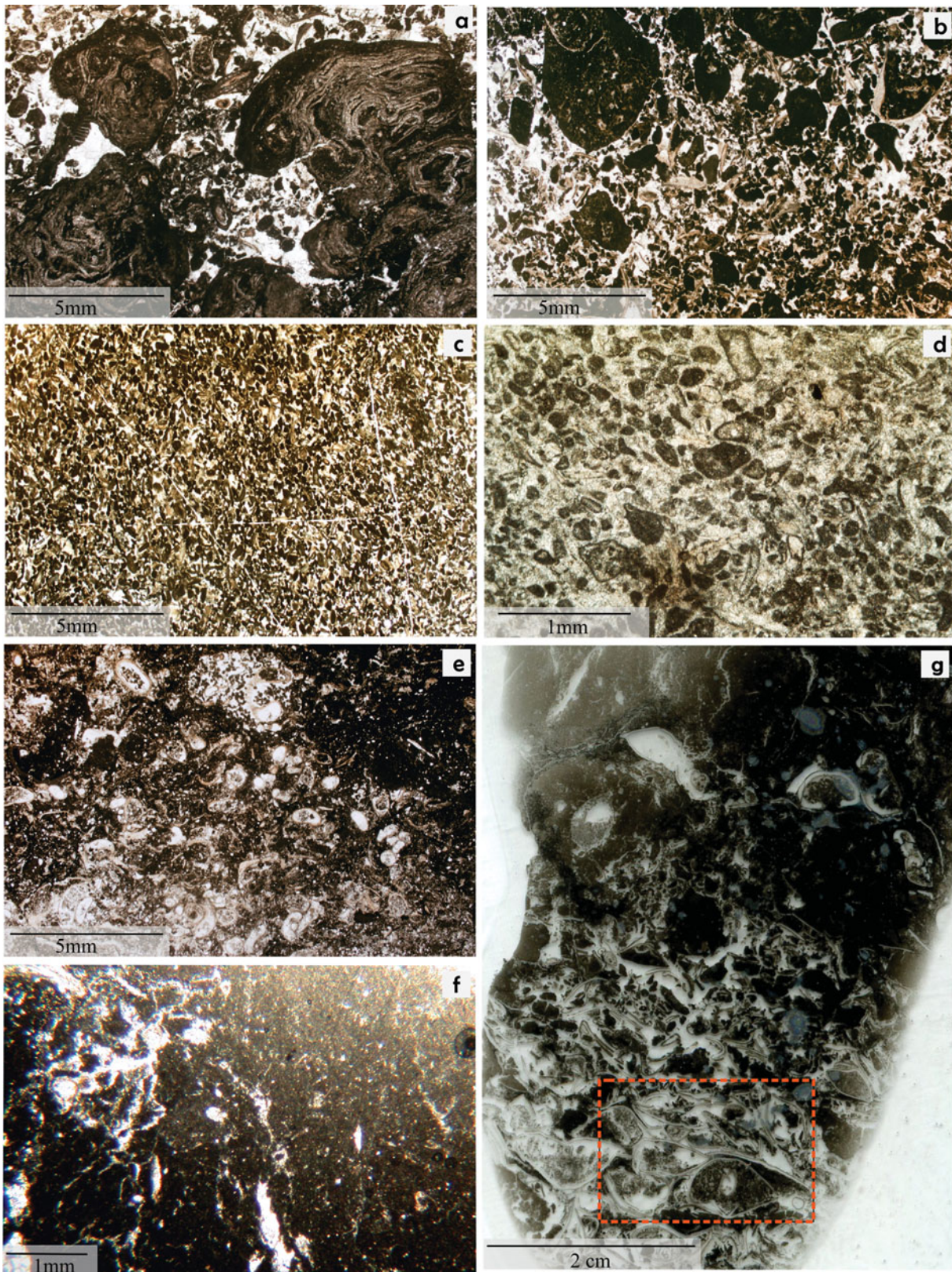


Figure 5. (Colour online) Microfacies RS2-LT3–4 and RS3-LT5 from the Givetian of the La Thure section, Belgium. Photomicrographs of thin-sections are oriented perpendicular to the bedding. Numbers preceded by ‘TUR’ correspond to bed numbers. (a) RS2-LT3 bioclastic shoals: calcimicrobe *Sphaerocodium* oncoidal grainstone–rudstone (TUR 200b, transmitted light). (b) RS2-LT3 bioclastic shoals: lithoclastic grainstone–rudstone (TUR 189, transmitted light). (c) RS2-LT4 bioclastic shoals: fine-grained peloidal bioclastic grainstone (TUR 163c, transmitted light). (d) RS2-LT4 bioclastic shoals: peloidal grainstone with mud-coated grains (TUR 138b, transmitted light). (e) RS3-LT5 internal shelf with good circulation: wackestone showing worm tube accumulation (TUR 157, transmitted light). (f) RS3-LT5 internal shelf with good circulation: mudstone–wackestone with fenestrae (TUR 176, transmitted light). (g) RS3-LT5 internal shelf with good circulation: coarse-grained brachiopod shell level overlain by a fenestral mudstone–wackestone (TUR 176, scanned thin-section).

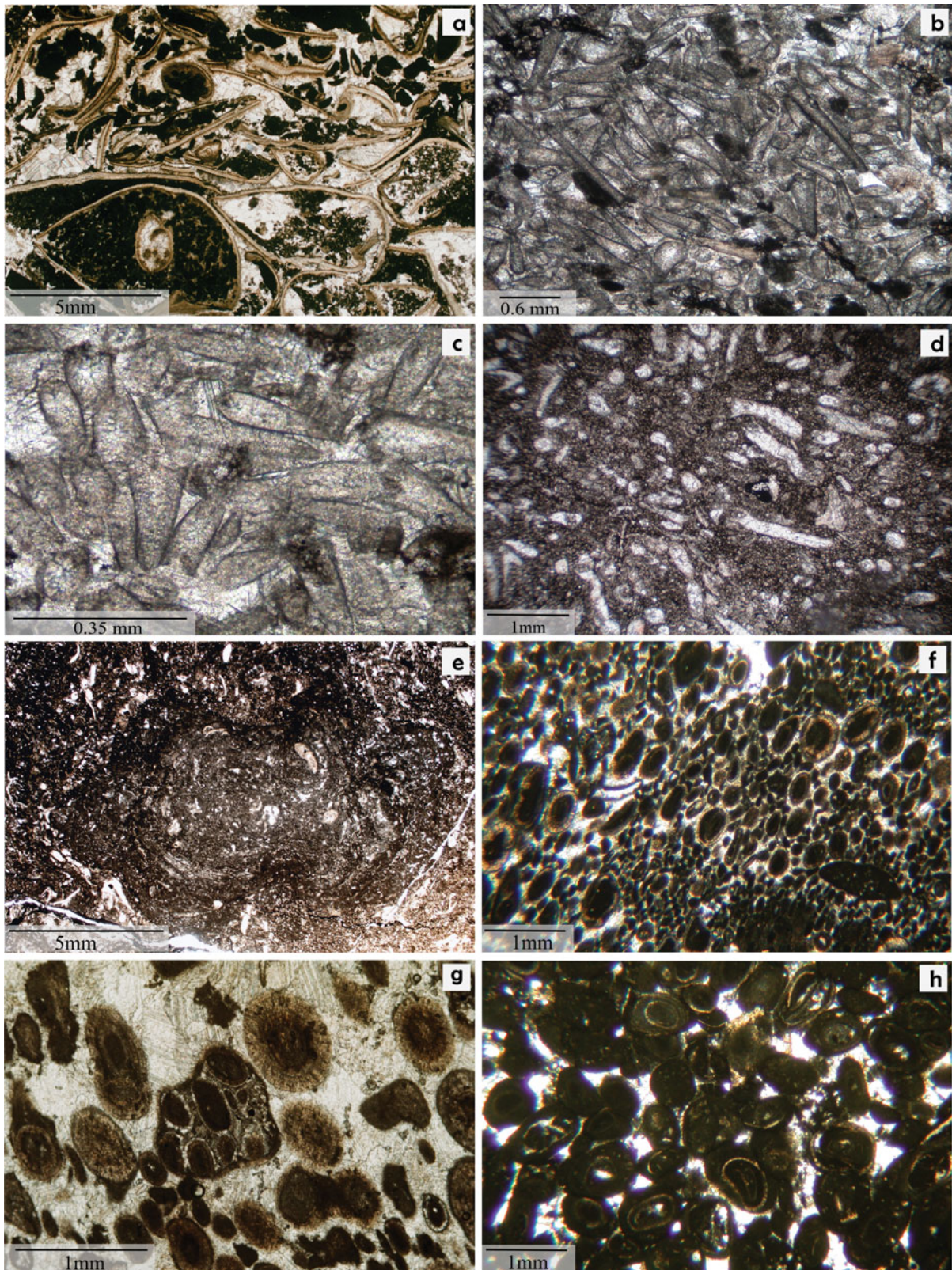


Figure 6. (Colour online) Microfacies RS3-LT5–8–10a and RS4-LT10b–c from the Givetian of the La Thure section, western Belgium. Photomicrographs of thin-sections are oriented perpendicular to the bedding and were all made in transmitted light. (a) RS3-LT5 internal shelf with good circulation: brachiopod shell rudstone showing whole shell filled by a clotted fabric (for location see inset in Fig. 5g) (TUR 176). (b) RS3-LT6 internal shelf with good circulation: whole ‘*Magnella*’ shell grainstone (TUR 133). (c) RS3-LT6 internal shelf with good circulation: focused on conical shells like ‘*Magnella*’ (TUR 133). (d) RS3-LT8 internal shelf with good circulation: dolomitized packstone rich in palaeoberesellid (TUR 149b). (e) RS3-LT8 internal shelf with good circulation: *Girvanella* oncoid within a rich issinellid packstone (TUR 156). (f) RS3-LT10a internal shelf shoal setting: moderately sorted oolitic grainstone (oolite Type 3) with common peloids (TUR 159c). (g) RS4-LT10a internal restricted shelf shoal setting: detail on Type 3 oolite (Strasser, 1986), peloids and aggregate grains within a moderately sorted oolitic grainstone (TUR 159a). (h) RS4-LT10b internal restricted shelf lagoonal setting: micritized oolite grainstone (oolites are mainly of Type 2 and 4 – TUR 180).

crofacies is the abundance of whole *Magnella* shells (i.e. attributed to pteropods by Neumann, Pozaryska & Vachard, 1975, pl. 3), associated with brachiopod shells. The *Magnella* shells are always complete, they show an average size of around 0.2 mm and can locally represent 80% of the sediment. Millimetre-sized brachiopod shells are mostly articulated but often strongly deformed. Space between organisms is filled with sparitic cement. Peloids are locally abundant; they are spread within the sediment or occur as millimetre-sized pockets. Where deformed brachiopod shells occur it is common to observe argillaceous seams and a pressure-solution fabric. Moulds of brachiopod shells are commonly filled with conical shells of *Magnella*. Rare lumps of *Girvanella* occur.

Interpretation

The characteristics of this microfacies point to an environment where energy is high enough to prevent the deposition of micrite (grainstone texture). The limited thickness of this microfacies and its intercalation with RS3-LT5 mudstone and wackestone suggest event-like deposition as tempestites. Indeed, overlying and underlying microfacies indicate a subtidal internal shelf setting. The scarcity of mentions of '*Magnella*' in the literature does not allow for the inference of further details on the ecological interpretation.

RS3-LT7: stromatoporoid rudstone

These rudstones are relatively similar to those described in RS1-LT2. Differences are mainly the absence of open-marine organisms, such as crinoids and trilobites, the occurrence of the branching tabulate *Stachyodes*, fasciculate rugose corals and frequent Paleosiphonocladales. Stromatoporoids are locally encrusted by *Sphaerocodium* and serpulids. As for RS1-LT2, the matrix is often dolomitized and rich in insoluble residues.

Interpretation

The occurrence of reef organisms encrusted by calcimicrobes and serpulids, and the occurrence of *Stachyodes* are in favour of back-reef and near-reef environments (Flügel, 2004, p. 500). Furthermore, the absence of crinoids and trilobites suggests limited connection to a fully marine setting. This microfacies could correspond to small patch-reefs developed in an internal shelf setting.

RS3-LT8: Paleosiphonocladales wackestone–packstone

The main characteristics of this microfacies are the dark colour of the sediment, the commonly dolomitized matrix and the abundance of variously preserved issinellid and palaeoberesellid algae (Fig. 6d). Other organisms are broken brachiopod shells, ostracods and locally millimetre-sized *Girvanella* oncoids (Fig. 6e), rugose corals and branching stromatoporoids. Shells commonly expose spongiostromate encrustation. Irregular millimetre-sized grainstone lenses rich in micritic lithoclasts occur locally.

Interpretation

The abundance of issinellids and palaeoberesellids in a wackestone to packstone texture suggests a relatively quiet setting in the vicinity of Paleosiphonocladales. In a paper dedicated to the Belgian Givetian platform, Mamet & Pr at (1986) established that these algae mostly occurred in barrier and lagoonal settings. Considering the absence of reefal organisms we suggest deposition in a location distant from reefal influence.

RS3-LT9: burrowed calciphere mudstone (Fig. 2b)

The main characteristic of this mudstone is the occurrence of frequent calcispheres floating in a dark-brown micritic matrix and the common occurrence of centimetre-sized vertical burrows filled with sparitic cement. Other organisms are rare and represented by palaeoberesellid algae, ostracod shells and pteropods like *Magnella* shells (see also RS3-LT6). Locally, millimetre-sized pockets displaying a clotted texture and small fenestrae are observed.

Interpretation

The abundance of micritic matrix and vertical burrows suggest a very quiet depositional setting likely located in a subtidal setting characterized by a low sedimentation rate, where settling is the main sedimentary process. Calcispheres are recognized as common constituents of Middle Devonian lagoonal and back-reef carbonate settings (Mamet, 1991; Fl ugel, 2004). Furthermore, the occurrence of palaeoberesellid algae is also in favour of a lagoonal setting. This microfacies is thus interpreted as being deposited in a lagoonal setting, likely above the FWFB but in a sheltered setting.

RS3-LT10a and RS4-LT10b–c: oolitic grainstone–packstone

This microfacies is characterized by the abundance of ooids and the good to moderate sorting of sediment. Based on the occurrence of various types of ooids (Type 1, 2, 3 and 4; Strasser, 1986), bioclast and lithoclast abundance, as well as texture, this microfacies can be divided into three categories: (RS3-LT10a) oolitic peloidal grainstone; (RS4-LT10b) oolitic lithoclastic grainstone–packstone and (RS4-LT10c) oolitic shelly packstone–wackestone.

RS3-LT10a: oolitic peloidal grainstone–packstone (Fig. 6f, g)

The main characters of this microfacies are the moderate to good sorting of sediment, the abundance (80–90%) of Type 3 and 1 ooids of Strasser (1986) and the regular occurrence of peloids. Type 1 corresponds to spherical micritic ooids with thinly laminated tangential cortices while Type 3 corresponds to ooids with thinly laminated fine-radial cortices. Observed ooids display an average size of 0.4 mm and are cemented by sparitic cement with the local occurrence of micritic matrix. The oolitic grainstone overlies RS3-LT5 mudstone–packstone with a sharp and erosional boundary. Lithoclasts of mudstone occur within the lower part of the overlying oolitic grainstone. Aggregate grains and micritic lithoclasts (infra-millimetre to millimetre-sized) are abundant and locally the space between ooids is dolomitized.

Interpretation

The abundance of well- to moderately sorted Type 1 and 3 ooids (Strasser, 1986) in a grainstone points to a depositional setting where water turbulence was relatively high, thus allowing for the sorting of grains, likely above the FWB. Furthermore, according to Strasser (1986), Type 1 ooids are formed in intertidal conditions with high water energy while Type 3 ooids (dominant) are interpreted as being formed within an intermittently agitated environment with moderate water energy (see fig. 10 in Strasser, 1986). This environment might correspond to an oolitic shoal or bar developed in a shallow lagoonal setting. Within his rimmed carbonate platform model, Wilson (1975) defined several standard microfacies (SMF) Types (e.g. SMF15) referring to the occurrence of shoals in a shelf interior. Occurrence of this microfacies overlying mudstone and wackestone (e.g. RS3-LT5) indicates that the suggested shoal was likely developed in an internal shelf setting, in the vicinity of microfacies RS3-LT5.

*Facies belt 4: internal restricted shelf**RS4-LT10b: oolitic lithoclastic grainstone–packstone (Fig. 6h)*

The main characteristics of this microfacies are the moderate sorting, the dominance of micritized Type 2 and 4 ooids (Strasser, 1986), and the occurrence of lithoclasts and bioclasts. Type 2 corresponds to irregular micritic ooids with thinly laminated cortices while Type 4 corresponds to ooids with a few fine-radial laminae. Observed ooids have an average size of around 0.5 mm and they commonly show a nucleus constituted either of micrite or broken shells. Lithoclasts, constituted either of mudstone or oolitic grainstone/packstone, are usually rounded and range from 0.3 to 7 mm in size. Other observed allochems are rare and correspond to aggregate grains and broken brachiopod/bivalve shells. When the matrix is micritic, the sorting is moderate to poor. Micritization of allochems is generally significant.

Interpretation

Type 2 ooids are formed within normal marine salinity conditions while Type 4 ooids are made within hypersaline conditions. However, both of these types of ooids develop in calm to moderately agitated water likely within a lagoonal environment (Strasser, 1986). In comparison to RS3-LT10a, especially in the case of the Type 4 ooids, this microfacies might be located in a more proximal setting than RS3-LT10a.

RS4-LT10c: oolitic shell packstone and wackestone (Fig. 7a)

This microfacies is mainly characterized by well to moderately sorted Type 4 ooids embedded in a micritic matrix (Fig. 7a). These oolites show ooids with an average size of around 0.4 mm with a micritic nucleus. The oolites are usually moderately packed but locally occur as densely packed oolitic levels, parallel to the bedding. Bioclasts consist only of broken bivalve and ostracod shells. This microfacies only occurs in the up-

per part of the Fromelennes Fm (U3), with RS5-LT14 and 15.

Interpretation

Type 4 oolite indicates restricted salinity conditions and intermittently agitated water conditions (Strasser, 1986). The abundance of micritic matrix resulting from mud settlement within calm water and the common occurrence of bivalve shells are in accordance with this interpretation. The local occurrence of this microfacies within the intraclastic breccia characterizing RS5-LT14 attests to restricted conditions during deposition.

In conclusion, submicrofacies RS3-LT10a, RS4-LT10b and RS4-LT10c were all deposited on shoals inside an internal shallow shelf setting in a context of various levels of water energy and restriction. From RS3-LT10a to RS4-LT10c the proximality or the restriction degree of the lagoon increased. The occurrence of the shoals in internal platform settings is also supported by the extended width of the internal platform (e.g. from the coastline to the barrier), estimated at about ~60 km by Pr  at (2006). This significant width, therefore, contributes to the development of a large range of hydrodynamic conditions.

RS4-LT11: lithoclastic rudstone (Fig. 7b)

This microfacies is characterized by variously sized (0.3 to 7 mm) angular to sub-rounded lithoclasts (Fig. 7b) cemented by sparitic cement. Lithoclasts are mainly composed of peloidal and oolitic grainstone (e.g. RS3-LT10a and RS4-LT10b–c) although locally, micritic lithoclasts can occur. A laminated fabric is underlined by the alternation of coarse- and fine-grained lithoclasts. Within the layers dominated by fine-grained lithoclasts abundant peloids occur. Type 1 and 3 ooids (Strasser, 1986) are commonly visible within the sediment and the fabric is clast-supported with blocky sparitic cement.

Interpretation

The rudstone texture and the abundance of oolitic grainstone (RS3-LT10a) and micritic lithoclasts indicate the reworking of microfacies RS3-LT10a likely during a rapid increase in water energy. The limited occurrence of those sediments attests to the event-like character of this microfacies, which can be related to stronger tidal currents or storms. The distinction between those two processes is not obvious but in general an increasing proximity to the coastline is marked by an increasing influence of tidal currents. Thus, the depositional setting of this microfacies might have been located in the vicinity of RS3-LT10a and related to a rapid increase in water energy caused by storm or tidal currents.

*Facies belt 5: internal evaporitic shelf**RS5-LT12: dendroid stromatoporoid rudstone–floatstone (Figs 2d, 7c, d)*

Centimetre-sized dendroid (*Stachyodes* and *Amphipora*) and bulbous stromatoporoids lying parallel to

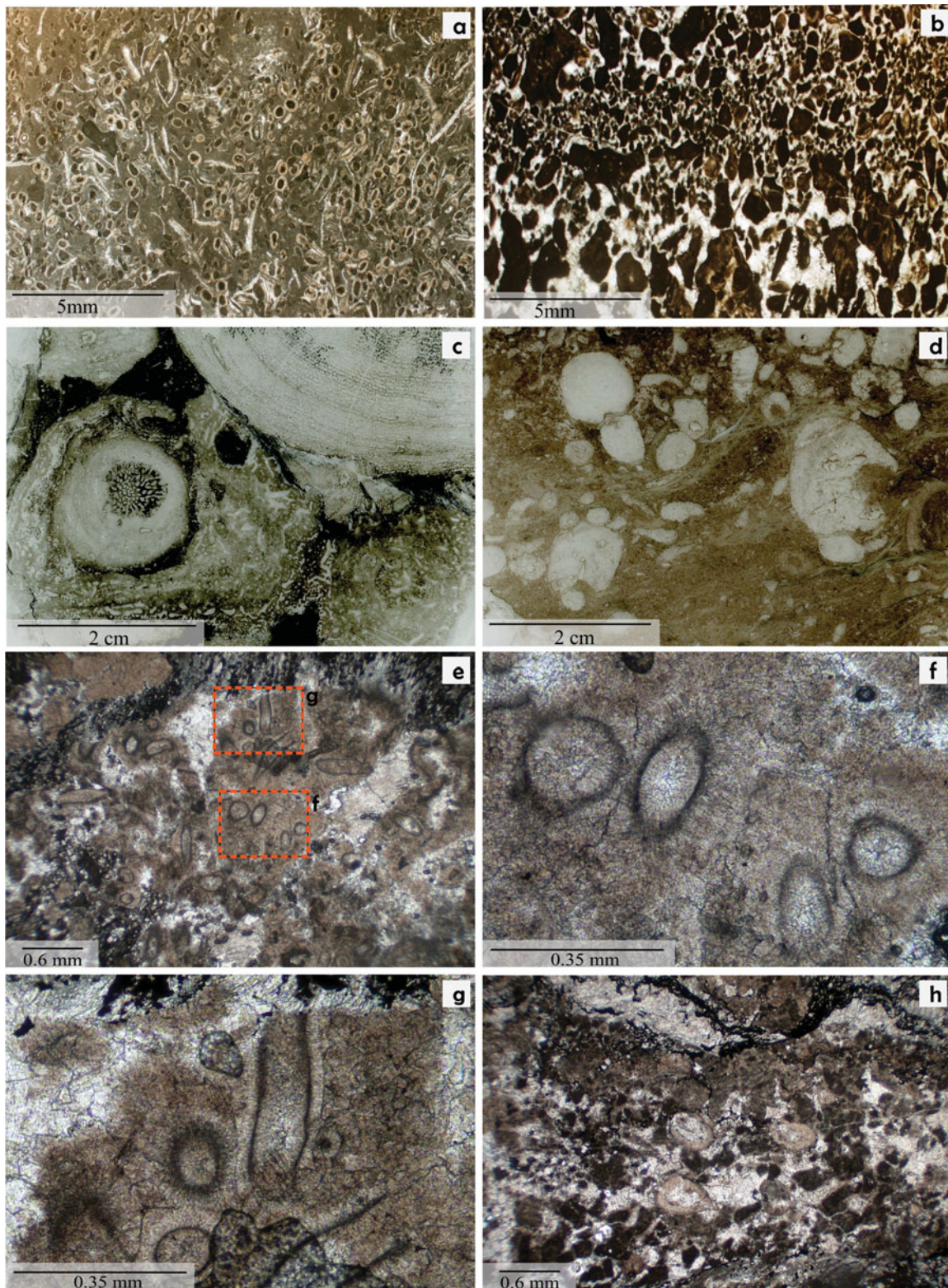


Figure 7. (Colour online) Microfacies RS4-LT10c–11 and RS5-LT12–13 from the Givetian of the La Thure section, western Belgium. Photomicrographs of thin-sections are oriented perpendicular to the bedding. (a) RS4-LT10c internal restricted shelf setting: wackestone–packstone with oolites (mainly of Type 4) and shells (TUR 268, transmitted light). (b) RS4-LT11 internal restricted shelf setting: coarse- to fine-grained lithoclastic rudstone–grainstone (large lithoclasts are constituted by oolitic grainstone) (TUR 226a, transmitted light). (c) RS5-LT12 internal evaporitic shelf setting: stromatoporoid rudstone (TUR 285, scanned thin-section). (d) RS5-LT12 internal evaporitic shelf setting: dendroid stromatoporoid rudstone (TUR 279c, scanned thin-section). (e) RS5-LT13 internal evaporitic shelf setting: boundstone (TUR 119, transmitted light). (f) RS5-LT13 internal evaporitic lagoonal setting: focused on micritic tubular structure with rims of fibrous cement (for location see inset in (e)) (TUR 119, transmitted light). (g) RS5-LT13 internal evaporitic lagoonal shelf setting: focused on the elongated tubular structure (note the polygonal aspect of the fibrous cement) (for location see inset in (e)) (TUR 119, transmitted light). (h) RS5-LT13 internal evaporitic shelf: peloidal and ostracod accumulation observed within RS5-LT13 algal boundstone (TUR 123a, transmitted light).

the bedding and fine-grained ocherous dolomitized matrix characterize this microfacies. *Stachyodes* are millimetre to centimetre in size and commonly show encrustation by millimetre-scale encrusting stromatoporoids. Rare moderately to poorly preserved allochems such as brachiopods, peloids, lithoclasts, *Girvanella*, *Renalcis* lumps, tabulate corals and unidentified bioclasts are observed between large organisms. Locally, centimetre-sized bulbous stromatoporoids can be frequent. The sediment is moderately to well sorted. Locally, this microfacies is intercalated with sediment from RS5-LT14 (laminated mudstone – peloidal grainstone) with a sharp and erosive lower contact (Fig. 2d).

Interpretation

According to several authors (P. Cornet, unpub. Ph.D. thesis, Univ. Catholique de Louvain, 1975; Pohler, 1998; Wood, 2000) *Amphipora* and *Stachyodes* are characteristic of shallow-water back-reef lagoonal settings and growth on soft substrate. The occurrence of abundant *Stachyodes* and *Amphipora* in a rudstone/floatstone texture intercalated with laminated mudstone RS5-LT14 (defined below) suggests significant reworking of dendroid stromatoporoids, which grew in the relative vicinity of the RS5-LT12 and RS5-LT14 depositional settings. According to Flügel (2004, p. 500) branching stromatoporoids are frequently swept into other environments by storms. Furthermore, local erosive bases at the boundaries between RS5-LT14 and RS5-LT12 and the good sorting of dendroid stromatoporoids indicate an important increase in water energy enabling the reworking and landward transport of stromatoporoid patch-reefs within a location characterizing RS5-LT14.

RS5-LT13: algal microbial boundstone (Figs 7e–h)

This microfacies occurs in the lower portion of the Mont d'Hairs Fm and overlies beds formed by RS5-LT14. It is mainly characterized by the numerous occurrences of micritic tubular structures (diameter of tubes is around 0.2 mm), the abundance of cement and the common occurrence of peloids arranged in a clotted fabric. Locally, ostracods (showing thick-walled valves) and recrystallized worm tubes occur. Thin micritic tubes are usually surrounded by a fringe of fibrous cement (Fig. 7f, g) which fills the interparticle pores. This microfacies is also characterized by numerous stylolitic seams rich in insoluble residues locally forming a 'horse-tail' structure and on a larger scale an iden-supported fabric.

Interpretation

The abundance of sparitic cement and clotted fabric is in favour of a microbial/bacterial mediation (e.g. thrombotic fabric: 'peloidal micrite', exhibiting a distinct clotted fabric; Flügel, 2004, p. 86). The abundance of sparitic cement filling the interparticle pores between thin micritic walled tubes is in favour of a relatively shallow-marine protected setting allowing the development of these thin tubes. Given the diameters of the micritic tubes (~2 mm), they would have been

destroyed by any energetic event. According to Stepko Golubic (pers. comm.), the diameters of these tubes are out of the size range for cyanobacteria. Intercalation of this microfacies with RS5-LT14, interpreted as a lagoonal restricted environment, suggests an internal evaporitic setting for this microfacies.

RS5-LT14: laminated mudstone – peloidal grainstone

(Fig. 8a–f)

One of the most specific characteristics of this microfacies is the common occurrence of both wrinkled and regular laminae (Fig. 8a) underlined by a couplet of micrite alternating with fine-grained peloidal grainstone (Fig. 8b). Laminae can be arranged either in dense or sparse growth patterns (millimetre- to centimetre-sized). Within grainstone layers, the sizes of the peloids are relatively homogeneous, although from one layer to the next it can vary substantially (0.1 to 2 mm). Millimetre-sized vertically pronounced fenestral fabrics (Fig. 8a) crossing lamination and fenestrae showing horizontal patterns occur in this microfacies. Dolomitization is common and when affecting the sediment, the laminae are less clearly visible. Lamination can be locally highlighted by silt-sized quartz-grain-rich layers alternating with micritic-rich layers (Fig. 8c). Occasionally, lamination displays millimetre-scaled protuberances (Fig. 8d) locally filled with coarse calcite cement (Fig. 8e). Issinellids and *Amphipora* fragments floating in micritic mud (Fig. 8f) and gypsum evaporitic pseudomorphs are also observed. In this microfacies, fine-grained micritic clast grainstone layers occur locally and silt-sized quartz grains and clays are occasionally an important constituent of the sediment.

Interpretation

The abundance of laminae (locally wrinkled), the occurrence of fenestrae and peloids and fine-grained micritic matrix characterize microbially modified sediments (Aitken, 1967). In the Middle Devonian carbonate platform of Poland, Skompski & Szulczewski (1994) interpreted similar microfacies as having formed within the shallow intertidal to supratidal restricted shelf. Similar upper Givetian sediments in Belgium are interpreted as having been deposited in extensive tidal flat complexes including channel, levee and back-levee systems (see microfacies Type 1', 2' and 3' and fig. 7 of Boulvain & Pr at, 1986). Furthermore, the occurrence of laminae crossed by a vertical fenestral fabric corresponding to desiccation cracks and the occurrence of evaporitic pseudomorphs both point to a setting temporarily subjected to emersion and an arid climate, triggering the desiccation of soft sediments. According to Scholle & Ulmer-Scholle (2003, p. 6) and Purser (1980, p. 98), laminae protuberances relate to the growth of evaporitic minerals (e.g. anhydrite) within the sediment. The rare occurrence of fauna corresponds to a hostile evaporitic environment and is characteristic of an inter- to supratidal restricted evaporitic setting.

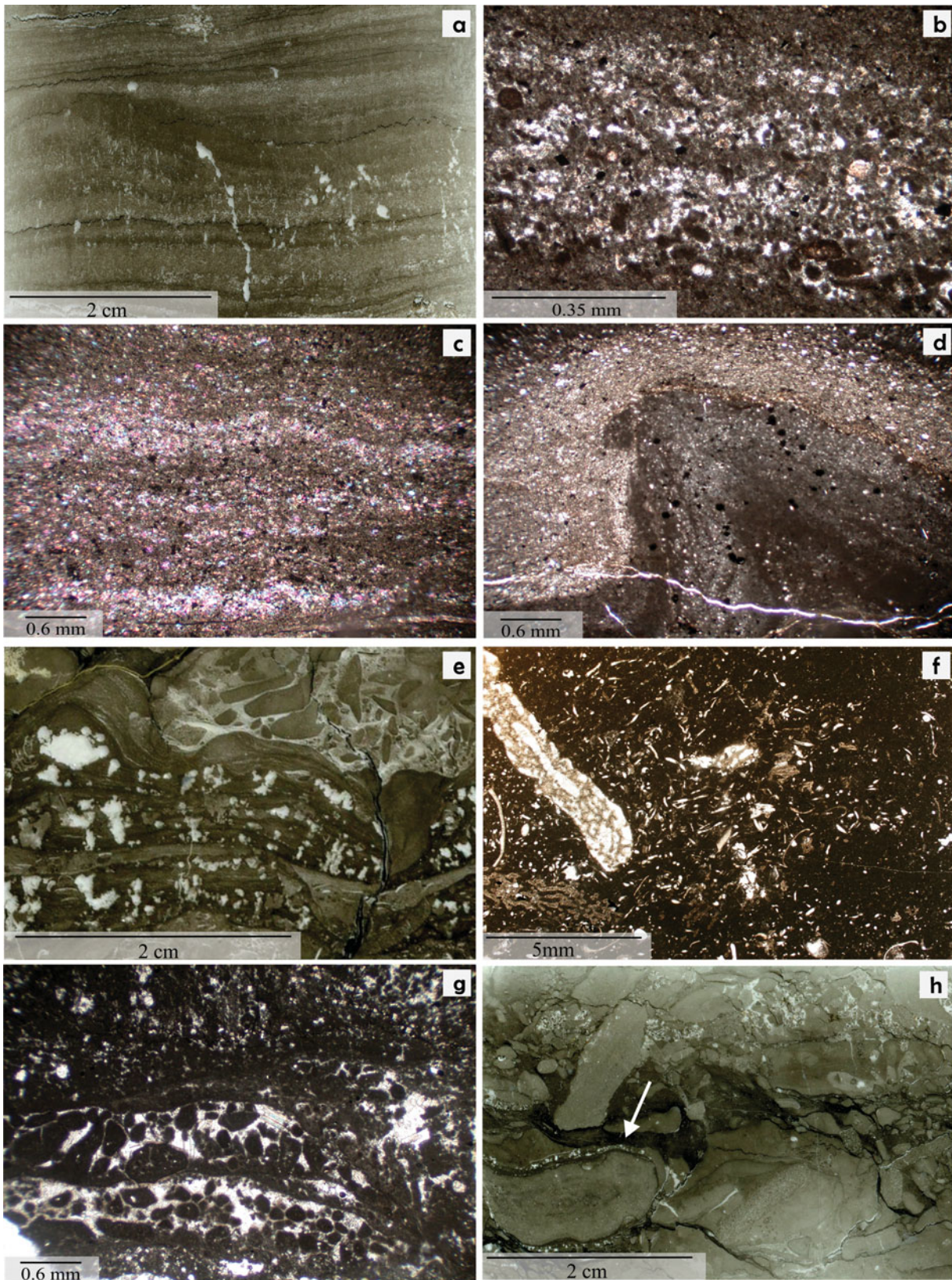


Figure 8. (Colour online) Microfacies RS5-LT14 and RS5-LT15 – inter- to supratidal internal evaporitic shelf – from the Givetian of the La Thure section, western Belgium. Photomicrographs of thin-sections are oriented perpendicular to the bedding. (a) RS5-LT14: alternation of dark and lighter laminae locally crossed by vertical fenestriae (TUR 158, scanned thin-section). (b) RS5-LT14: fine-grained peloidal grainstone alternating with mudstone texture (TUR 287, transmitted light). (c) RS5-LT14: alternation between silt-sized quartz-rich and micritic-rich levels (TUR 117, crossed light). (d) RS5-LT14: laminae marked by a well-developed protuberance (TUR 117, transmitted light). (e) RS5-LT14: wrinkled laminae showing stacked protuberance filled by coarse calcite cement (note the intraclastic breccia in the upper right of the thin-section) (TUR 293b, scanned thin-section). (f) RS5-LT14: abundant palaeoberesellids floating in a micritic matrix (TUR 282, transmitted light). (g) RS5-LT15: partly reworked algal mat (TUR 120, transmitted light) (h) RS5-LT15: intraclastic grainstone–rudstone (note the lithoclasts surrounded by algal layer) (TUR 291d, scanned thin-section).

RS5-LT15: intraclastic rudstone–grainstone (Figs 2d, 8g, h)

This microfacies is characterized by the millimetre- to centimetre-sized angular to rounded-elongated fenestral mudstone lithoclasts. Lithoclasts are locally surrounded by wrinkled laminae and space between lithoclasts is filled either by ooids, clay or coarse-grained sparitic cement. Pressure-solution processes produced iden-like textures.

Interpretation

Millimetre- to centimetre-sized elongated fenestrae associated with mudstone lithoclasts, corresponding to lithified algal mats, indicate the reworking of supratidal deposits likely during an increase in water energy (e.g. storms). The wrinkled laminae surrounding the lithoclasts argues for re-deposition in intertidal to supratidal settings. Oolites are likely allochthonous and derived from an oolitic sand bar located seawards (e.g. RS3-LT10a). Skompski & Szulczewski (1994, pl. 49) interpreted relatively similar deposits as tide-channel breccias. This microfacies might thus be deposited within an upper intertidal to supratidal location (e.g. tidal flat) and related to a change in the water energy triggering a reworking of the sediment and the transport of oolites through the RS5-LT15 depositional setting.

4.c. Summary of microfacies interpretation: palaeoenvironmental model (Table 1; Fig. 9)

Field and petrographic analyses of the La Thure section led to the definition of 18 microfacies (Table 1). These microfacies are an outstanding example of the wide range of depositional settings that shaped a shallow carbonate platform during early to late Givetian time. Together, these microfacies represent different types of carbonate platform setting and show a remarkable evolution through early to late Givetian time. Following the definition of Read (1985), we distinguish three main platform profiles for the La Thure section: (1) a homoclinal ramp (RP-LT1–2); (2) a shallow-water discontinuously rimmed shelf (RS1–5–LT1–15); and (3) a drowning shelf (DS-LT1) (Fig. 9a). The establishment and differentiation between the three sedimentological models is based on the combination of field and microfacies criteria (e.g. marked lithological changes, faunal assemblage, matrix nature, terrigenous content and sediment texture) and the abundant literature mentioned throughout the previous sections. A major criterion for the establishment of the rimmed shelf profile on the western margin of the Dinant Syncline during middle Givetian time is the significant occurrence of biostromal deposits interpreted as having originated from a barrier-reef (G. Poulain, unpub. Masters thesis, Univ. Liège, 2006; Boulvain *et al.* 2009), in time-equivalent lithologies on the southern margin.

The carbonate ramp model of the La Thure section includes mid- and outer-ramp settings. Bioclastic lime mudstone to packstone (RP-LT1) and crinoidal packstone–grainstone (RP-LT2) characterize the mid- and outer-ramp settings and are interpreted as having

been deposited above the FWB but within the storm wave zone. Inner-ramp deposits are not observed in the La Thure section. For the rimmed shelf profile the situation is more complex. Indeed, in order to underline the diversity of depositional settings we divided this profile into five facies belts (RS1–RS5). These belts extend from an external fore-reef and biostrome to a supratidal internal shelf setting. Open-marine bioclastic wackestone–packstone (RS1-LT1) and coral–stromatoporoid rudstone–floatstone (RS1-LT2) represent the most distal settings defined on this shelf. Calcimicrobial bio-lithoclastic grainstone (RS2-LT3) and peloidal–lithoclastic grainstone with gastropods (RS2-LT4) correspond to sediments recorded in the bioclastic shoals developed at the platform interior margin (RS2). In a landward location, the internal shelf with good circulation (RS3) is characterized by a large set of microfacies: (a) mudstone to packstone with lithoclastic–brachiopod rudstone–grainstone layers (RS3-LT5), (b) *Magnella* shell grainstone and rudstone (RS3-LT6), (c) stromatoporoid rudstone (RS3-LT7), (d) Paleosiphonocladales wackestone–packstone (RS3-LT8), (e) burrowed calcisphere mudstone (RS3-LT9) and (f) oolitic peloidal grainstone–packstone (RS3-LT10a). Oolitic lithoclastic grainstone–packstone (RS4-LT10b), oolitic shell packstone and wackestone (RS4-LT10c) and lithoclastic rudstone (RS4-LT11) characterize the internal restricted shelf belt (RS4). Dendroid stromatoporoid rudstone–floatstone (RS5-LT12), algal microbial boundstone (RS5-LT13), laminated mudstone – peloidal grainstone (RS5-LT14) and intraclastic rudstone–grainstone (RS5-LT15) correspond to the most proximal facies belt (RS5) defined in this carbonate shelf model. The drowning shelf model is characterized by mudstone and wackestone with densely packed brachiopod–bivalve shell levels (DS-LT1). Microfacies stacking patterns for the Givetian interval in the La Thure section permit recognition of five main depositional intervals (I–V) separated by noteworthy shallowing–deepening trends in the section. The two first intervals correspond, respectively, to the Terre d’Hairs and Mont d’Hairs formations while the last three fit with the three lithological units defined for the Fromelennes Fm.

4.d. Magnetic susceptibility

In order to apply MS as a palaeoenvironmental proxy or as a tool for correlation, it is necessary to assess whether the MS signal reflects primary depositional conditions or secondary post-depositional imprint (synthesis in Da Silva *et al.* 2013). This assessment is imperative in our case as Devonian rocks from Belgium underwent a remagnetization event driven by the Variscan orogeny (Zegers, Dekkers & Baily, 2003; Zwing *et al.* 2005). In a recent study dedicated to the origin of the MS signal in Devonian sections of Belgium, Da Silva *et al.* (2012, 2013) established that the MS signal is mainly carried by fine-grained pseudo-single domain (PSD) magnetite formed during this remagnetization event.

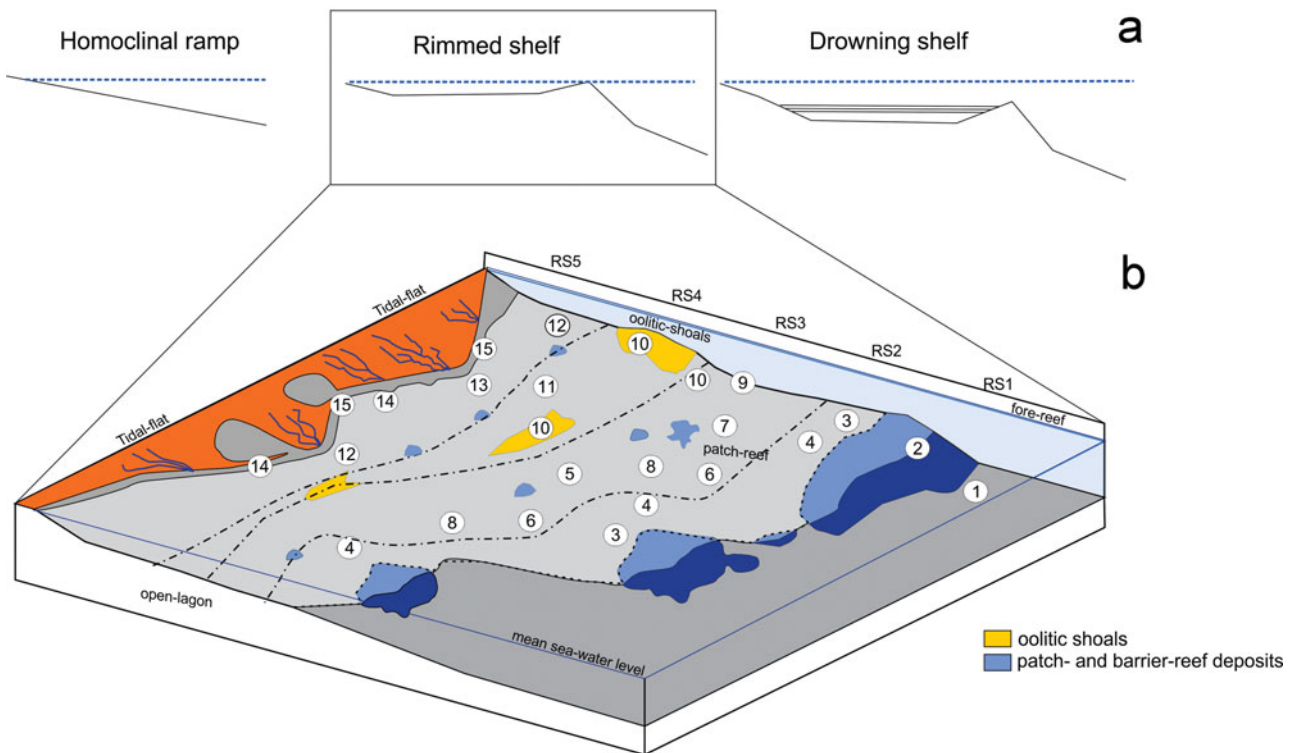


Figure 9. (Colour online) (a) Homoclinal ramp, rimmed shelf and drowning shelf profiles of carbonate platform models proposed for the deposits observed in the La Thure section. (b) Detail of the main facies belts defined into the carbonate shelf model.

Nevertheless, Da Silva *et al.* (2013) also showed that of six Devonian outcrops, four of them were still reflecting variations in detrital input as indicated by the relatively good relationship between MS and siliciclastic input proxies such as Ti, Zr, Al and Si. Similar results for the Devonian of western Belgium were recently published by Pas *et al.* (2015).

The MS values for the lower–upper Givetian part of the La Thure section range between -5.64×10^{-9} and $2.97 \times 10^{-7} \text{ m}^3/\text{kg}$ with an average value of $4.15 \times 10^{-8} \text{ m}^3/\text{kg}$. The entire MS curve provided for the Givetian of the La Thure section can be divided into six main MS units (MSU-I–MSU-V; Fig. 10). A vertical dotted line indicates the average MS value for each MS unit on Figure 10. The six main MS units correspond to the sedimentary intervals established from the microfacies curve. The Terre d’Hairs Fm shows locally relatively high values ($1.5 \times 10^{-7} \text{ m}^3/\text{kg}$) and an average close to $1 \times 10^{-7} \text{ m}^3/\text{kg}$ (MSU-I). The overlying Mont d’Hairs Fm records the lowest average MS value ($0.2 \times 10^{-7} \text{ m}^3/\text{kg}$; MSU-II) and is locally punctuated by peaks reaching $1.3 \times 10^{-7} \text{ m}^3/\text{kg}$. A particularity of MSU-II is the occurrence of some well-defined cycles recorded in the MS curve. In this internal shelf setting MS values are homogeneous and relatively low. Higher up in the section, within the base of the Fromelennes Fm, MS values increase and show an average value of $0.75 \times 10^{-7} \text{ m}^3/\text{kg}$ (MSU-III). Locally, peaks reaching $1 \times 10^{-7} \text{ m}^3/\text{kg}$ also occur. The middle portion of the Fromelennes Fm, interval IV, shows lower mean values ($0.3 \times 10^{-7} \text{ m}^3/\text{kg}$; MSU-IVa) but, throughout the upper part of the Fromelennes Fm (up-

per part of Unit 2) these values increase rapidly and reach $3 \times 10^{-7} \text{ m}^3/\text{kg}$. Within this portion, the MS values oscillate strongly between 0.7 and $3 \times 10^{-7} \text{ m}^3/\text{kg}$ (MSU-IVb). Then values decrease to reach intermediate values of $0.9 \times 10^{-7} \text{ m}^3/\text{kg}$ (MSU-V) within the uppermost portion of the Fromelennes Fm corresponding to Unit 3.

5. Discussion

5.a. Depositional environments: carbonate platform evolution

The transition between the carbonate ramp and the carbonate shelf model is characterized by lithological and microfacies changes (Fig. 10). Indeed, from 0 to 7.5 m, the Terres d’Hairs Fm is mainly characterized by black to brown argillaceous centimetre- to decimetre-thick limestone containing local accumulations of crinoids and brachiopods (for more details see description of the formations in Section 4). Above 7.5 m, the lithology is characterized by well-bedded dark decimetre-thick limestone with varying amounts of bioclasts such as gastropods, which corresponds to the Mont d’Hairs Fm. This lithological change corresponds to a transition from open-marine faunal assemblages to a shallow-water shelf setting. At the top of the studied section, the transition between the discontinuously rimmed shelf and the drowning shelf model is mainly based on a significant change that occurs within the uppermost part of the Fromelennes Fm (within Unit 3). Indeed, at the 150 m thick mark, there is a transition from lam-

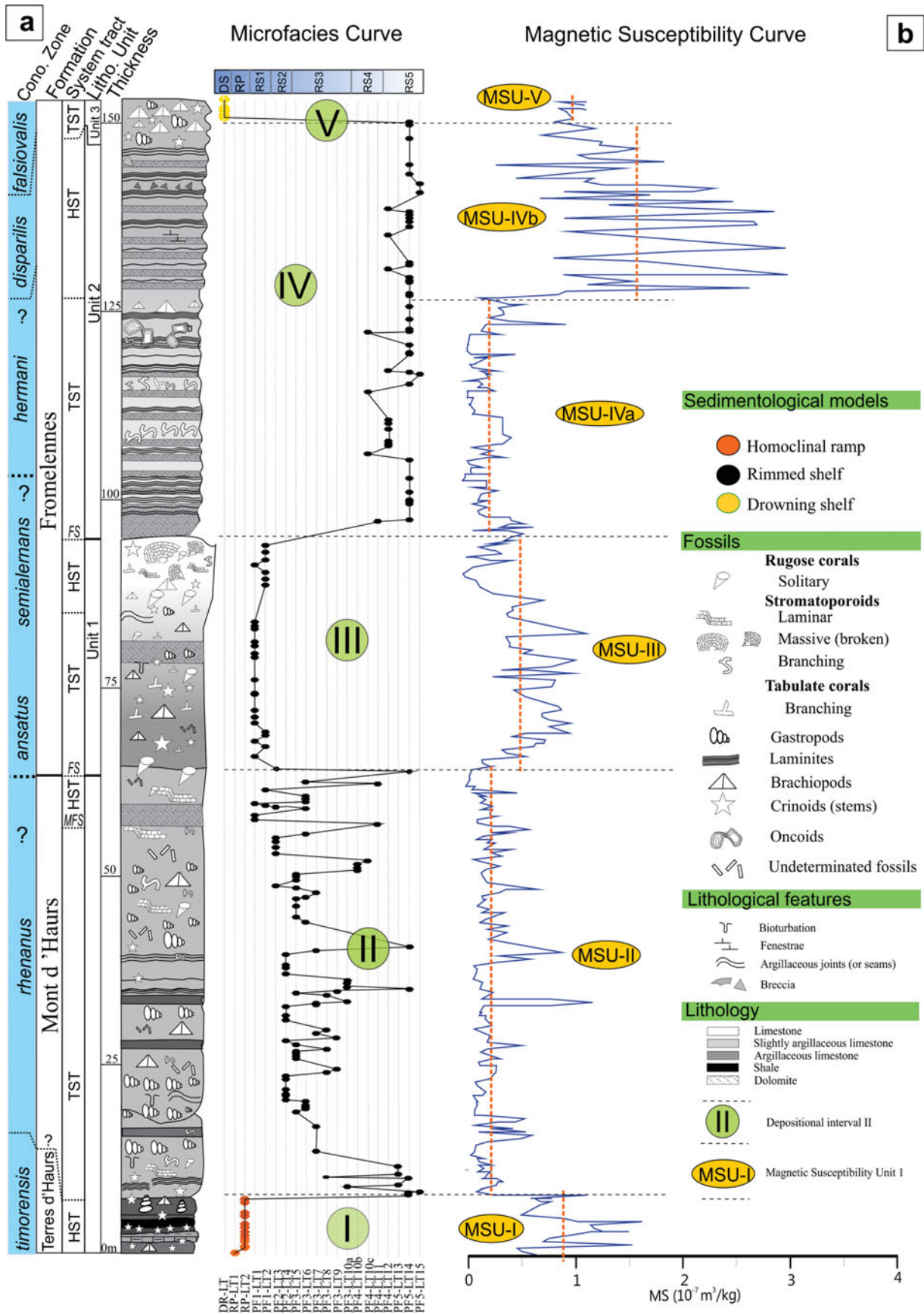


Figure 10. (Colour online) (a) Schematic sedimentological log showing formations, lithological units (U1–U3), system tracts and microfacies curve with the five main depositional intervals (I–V; intervals are separated by horizontal dotted lines). (b) Magnetic susceptibility evolution showing the six main magnetic susceptibility units (MSU-I to MSU-V). Vertical dotted lines correspond to average MS values for each MS interval.

inated limestone (RS5-LT14) to thicker and dark-blue bedded limestone containing numerous shells of brachiopods and debris of crinoids (DS-LT1), undoubtedly indicating re-establishment of open-marine conditions. This transition is interpreted as the result of a sea-level rise allowing restoration of open-marine conditions within an inter- to supratidal lagoonal setting, corresponding to the drowning shelf model. It is characterized by a wide spectrum of textures ranging from mudstone–wackestone to packstone–rudstone showing crinoids and shell accumulations (DS-LT1). These sediments are interpreted as having been deposited in an open-marine setting where the low rate of sedimentation allowed accumulation of shells and the development of a strongly bioturbated fabric. After 3 m of condensed shelly limestone, those limestones are overlain by ocherous limestone interlayered with black carbonaceous limestone and then brown shale belonging to the Nismes Fm of Frasnian age (for more detail about this transition see Pas *et al.* 2015).

In order to gain a better comprehension of the platform development during the early to late Givetian interval and to build a robust pattern for correlation we defined a microfacies curve for the La Thure section. Over the lower–upper Givetian, five main depositional intervals (I–V) separated by noteworthy shallowing–deepening trends are evident (Fig. 10). Based on this study and selected literature (Boulvain & Pr at, 1986; Pr at, Ceuleneer & Boulvain, 1987; Pr at & Boulvain, 1988; Bultynck *et al.* 1991; Boulvain *et al.* 1995, 2009; Pr at, 2006; Pr at & Bultynck, 2006; Maillet, Milhau & Pinte, 2011; Maillet, Milhau & Dojen, 2013) we illustrate the geometry and the key depositional changes characterizing the Givetian platform in the Dinant Basin. A summary of our interpretations and the illustration of the palaeogeographic history for the Dinant Basin during early to late Givetian time, including southward–northward migration of reefal bodies, is shown in Figure 11. Considering that the shallowest depositional settings in the Dinant Basin are located to the north, sedimentary rocks from the La Thure section, cropping out on the northwestern margin of the Dinant Syncline, must have been deposited in shallower settings than sediments belonging to the southern margin (e.g. Givet area; see geological map in Fig. 1b). The base of the Terre d’HOURS Fm (Fig. 11-I), deposited in the *timorensis* Zone, represents a carbonate ramp setting which is commonly observed prior to the extensive middle–late Givetian carbonate platform development in Belgium (Boulvain *et al.* 2009; Casier *et al.* 2013). The transition from the Terre d’HOURS to Mont d’HOURS formations (Fig. 10) is characterized by a shallowing–upward trend corresponding to a shift from mid-ramp (interval I) to internal shelf (interval II). This abrupt transition can be explained in the context of the well-marked north to south deepening of the depositional settings that are recorded for the Dinant Syncline (Pr at & Boulvain, 1988; Bultynck *et al.* 1991; G. Poulain, unpub. Masters thesis, Univ. Li ge, 2006; Pr at & Bultynck, 2006; see also Fig. 1d). At the south-

ern margin of the Dinant Syncline extensive biostromes developed throughout the Mont d’HOURS Fm (Boulvain *et al.* 2009; Casier & Pr at, 2013). The progressive development of large patches and barrier-reefs resulted in the formation of the thick-bedded limestone composed of reef-building organisms of the Mont d’HOURS Fm on the southern margin of the Dinant Syncline (cf. G. Poulain, unpub. Masters thesis, Univ. Li ge, 2006; Boulvain *et al.* 2009). These reefal structures must have progressively divided the middle Givetian platform into an internal and an external shelf setting (Fig. 11-II). These conditions created the sedimentary settings which allowed for the deposition of lagoonal and bioclastic shoal facies (e.g. RS2-LT3 to RS4-LT10) in the La Thure area. According to Boulvain *et al.* (2009), thick-bedded reefal limestones occurring throughout the Mont d’HOURS Fm within the southern margin of the Dinant Syncline are the result of gravity flows coming from a barrier-reef located northwards. With respect to this interpretation, the location of the barrier-reef separating the northwestern margin (La Thure) and the southern margin (Givet area; see map in Fig. 1b) of the Dinant Syncline might exist in the subsurface near the axis of the Dinant Syncline. The Mont d’HOURS Fm as exposed in the La Thure section records numerous oscillations of microfacies, which correspond to alternation of small-scale regressive cycles that may correspond to parasequences (see Fig. 10 interval II). As mentioned by several authors (Playford, 1980; F. Tourneur, unpub. Ph.D. thesis, Univ. Catholique de Louvain, 1985; Boulvain & Pr at, 1986; Pr at & Carliez, 1994; Skompski & Szulczewski, 1994; Da Silva & Boulvain, 2004; Boulvain *et al.* 2009), the record of cyclic sedimentation is a common characteristic of Devonian shallow-marine sequences. Moreover, De Vleeschouwer *et al.* (2015, see their fig. 3) related the 6 to 8 m thick oscillations in the microfacies curve to 100 ka eccentricity. At a larger scale, the Mont d’HOURS Fm can be considered as aggradational sedimentation in an inner-shelf setting.

The transition from the second (II) to the third interval (III) (Fig. 10) is characterized by a deepening–upward trend leading to the occurrence of biostromal and fore-reef deposits (RS1-LT1-2) in the La Thure area (Fig. 11-III), that overlie the inner-shelf and bioclastic shoal sediments (RS2-LT3 to RS4-LT10c) of the Mont d’HOURS Fm. This abrupt shift between intervals II and III is interpreted as the lateral equivalent of the transgressive pulse highlighted in the southern margin of the Dinant Syncline by Boulvain *et al.* (2009). In the Fromelennes type area, on the southern margin of the Dinant Syncline, this transgressive trend is marked by the occurrence of argillaceous limestone with an intercalation of clay (Pr at & Bultynck, 2006) overlying thick reefal limestone of the Mont d’HOURS Fm. However, with respect to the northwestern location of the La Thure section, this transgressive pulse must have been represented by shallower sedimentation than on the southern margin. As recently established by Narkiewicz, Narkiewicz & Bultynck (2015), this trans-

Early - Late Givetian carbonate platform development in Belgium

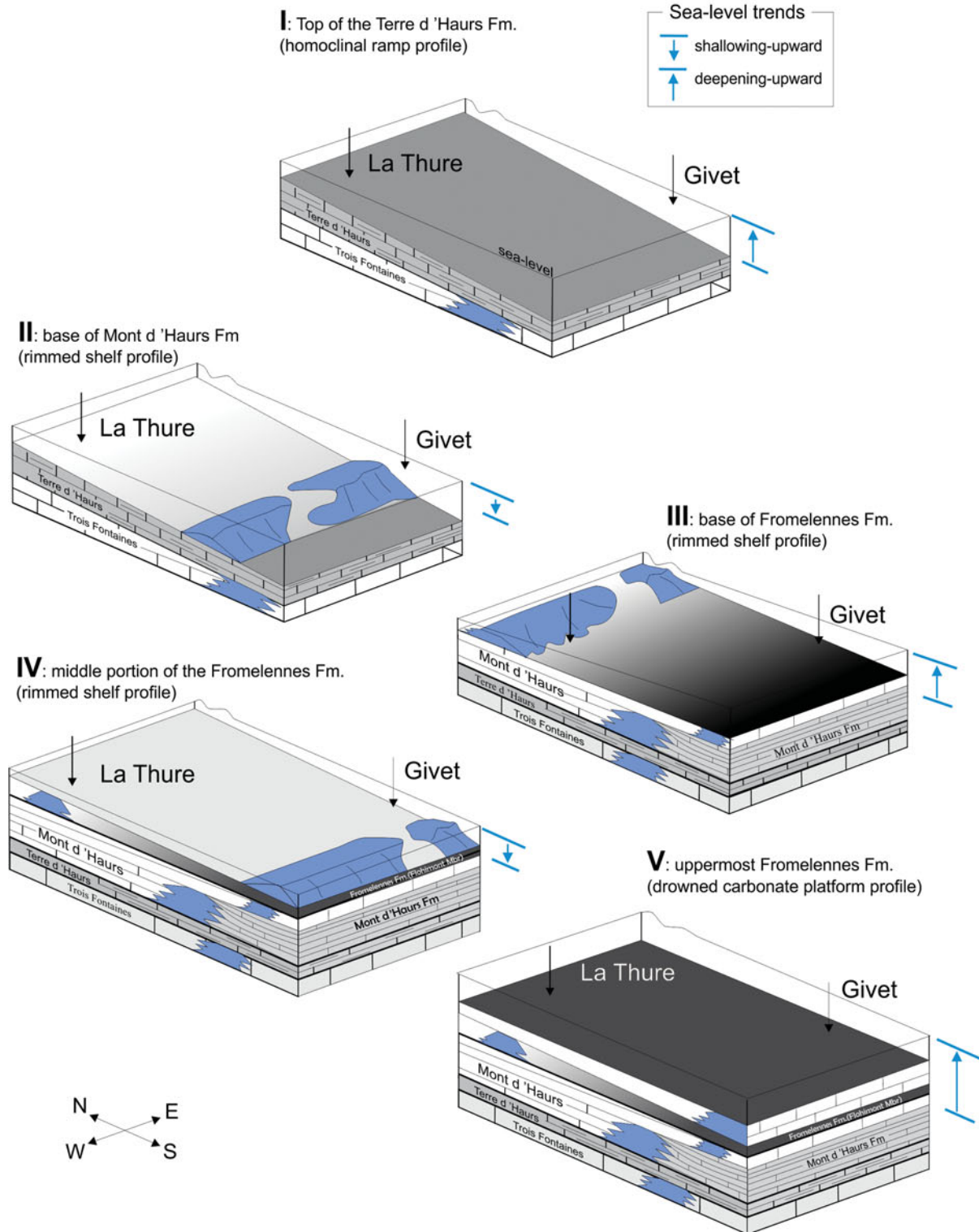


Figure 11. (Colour online) Early-late Givetian carbonate platform development within the Dinant Basin showing main basinward v. landward migration of the reefal body in relation to the sea-level variations.

gressive pulse in the base of the Fromelennes Fm (e.g. Flohimont Mbr) most likely corresponds to the base of the Taghanic Stage. Indeed, Narkiewicz, Narkiewicz & Bultynck (2015) recently reviewed conodont samples collected by Bultynck (1987) in the mid Givetian outcrop belt in the south of the Dinant Syncline and documented the presence of *P. ansatus* in the lowermost part of this formation. These new data led Narkiewicz, Narkiewicz & Bultynck (2015) to suggest that the transgressive basal part of the Fromelennes Fm corresponds to the base of the Taghanic Stage. The Taghanic Event is one of the most significant physical and biotic events of the Devonian associated with widespread transgression, the so-called Taghanic Onlap (Johnson, 1970) and major turnover in marine invertebrate and terrestrial vegetation (House, 2002; Aboussalam, 2003; Baird & Brett, 2008; Aboussalam & Becker, 2011; Marshall, Brown & Astin, 2011). Maillet, Milhau & Dojen (2013) also suggested the Taghanic biocrisis as a driving mechanism of the significant change in benthic ostracod diversity characterizing the basal part of the Fromelennes Fm in its type area (southern Dinant Syncline margin, France). Based on these lines of evidence, we suggest that the deepening shift at the base of interval III corresponds to the onset of the Taghanic Onlap in the northwestern Dinant Syncline.

As discussed above, interval II displays several small-scale sedimentary cycles interpreted as related to 100 ka eccentricity. In interval III, despite being a comparable thickness to interval II, no such cycles are visible in the microfacies. Absence of cycles in interval III might be an artefact related to the rapid development of reefal limestone. Indeed, reefal limestone can build up in the duration of a single small-scale cycle but related deposits are thick.

The transition from interval III to interval IV (Fig. 10) is marked by a drop in relative sea-level corresponding to the first occurrence of lagoonal deposits. This relative sea-level drop likely favoured a seaward shift of the reefal structure that had provided the materials deposited during interval III (e.g. biostromal and fore-reef deposits). The development of this reefal structure in a seaward location allowed initiation and deposition of lagoonal deposits landwards (e.g. analogous to the pattern discussed for the interval I to II transition; see also Fig. 11-IV). According to the research of several authors (Bultynck, 1974; Pr at & Carliez, 1994), synthesized in Boulvain *et al.* (2009), the mid-upper Givetian on the south and southeastern margin of the Dinant Syncline is also characterized by lagoonal sedimentation (e.g. Fromelennes Fm) and interpreted by Boulvain *et al.* (2009) as related to the occurrence of a barrier-reef located southwards. The occurrence of locally thick intervals of *Amphipora* rudstone (e.g. RS4-LT12; see microfacies Section 4) could indicate an important increase in the water energy in an internal lagoonal setting suggesting a discontinuous barrier. Interval IV locally shows the occurrence of small-scale regressive cycles similar to those described in Boulvain *et al.* (2009, p. 173). In the uppermost part of the

Fromelennes Fm (Fig. 10) the transition from interval IV to V corresponds to a significant deepening trend marked by the transition from lagoon-related (RS4–5 – LT12–15) to open-marine sedimentation (DS-LT1) including centimetre-sized brachiopods and crinoids. The lithostratigraphic position of this rapid transition, which is located a few metres below the first Frasnian shale (e.g. Nismes Fm; Pas *et al.* 2015) suggests that interval V is part of the large marine transgression characterizing the latest Givetian and the base of the Frasnian stage in Belgium.

5.b. Sequence stratigraphy

Based upon the previous discussion we have developed a preliminary sequential stratigraphic framework for the La Thure section. As presented above, the La Thure section is divided into five sedimentary intervals (I–V on Fig. 10) in which third-order systems tracts are recognized. Based on the abrupt shift towards shallower facies at the end of interval I, we can interpret this interval as a late highstand to falling stage. In interval II, two systems tracts are identified. The sedimentary sequence ranging from 9.5 m to 56 m in the measured section is identified as a transgressive systems tract (TST). The maximum flooding surface (MFS) is therefore located at the top of this TST and the remaining part of interval II corresponds to a highstand systems tract (HST). The base of interval III (64 m high) is a flooding surface (FS) that corresponding to the Taghanic Onlap. Interval III likely corresponds to a TST (from 64 to 88 m) followed by a HST (from 88 to 96 m) ending at the top of interval III. The top of interval III should correspond to a FS, which is associated with an emersion surface. This is followed by a new TST (from 96 to 131 m) enabling the accumulation of a thick sequence of peritidal facies and then likely a new HST that includes all the middle upper part of interval IV. Interval V clearly records a significant deepening of the facies which must correspond to a TST ending at the top of the section (153 m).

5.c. Comparison of magnetic susceptibility with selected geochemical elements

Detrital components such as Ti, Si, Th, Al and K are commonly used to document changes in siliciclastic input (Averbuch *et al.* 2005; Riquier *et al.* 2010; Śliwiński *et al.* 2012). For the La Thure section, we plot these elements next to the MS curve (Fig. 12). The large-scale trends followed by those elements show a moderate correlation with MS trends of the sample suite ($r = 0.51–0.61$; $n = 30$). These correlations indicate that the MS signal varies with the concentration of siliciclastic elements within the sediment. This means that variations in the terrestrial basinward influx have a strong influence on the intensity of the MS signal (for more examples see Da Silva *et al.* 2013). In addition, as mentioned for the Frasnian portion of this section (Pas

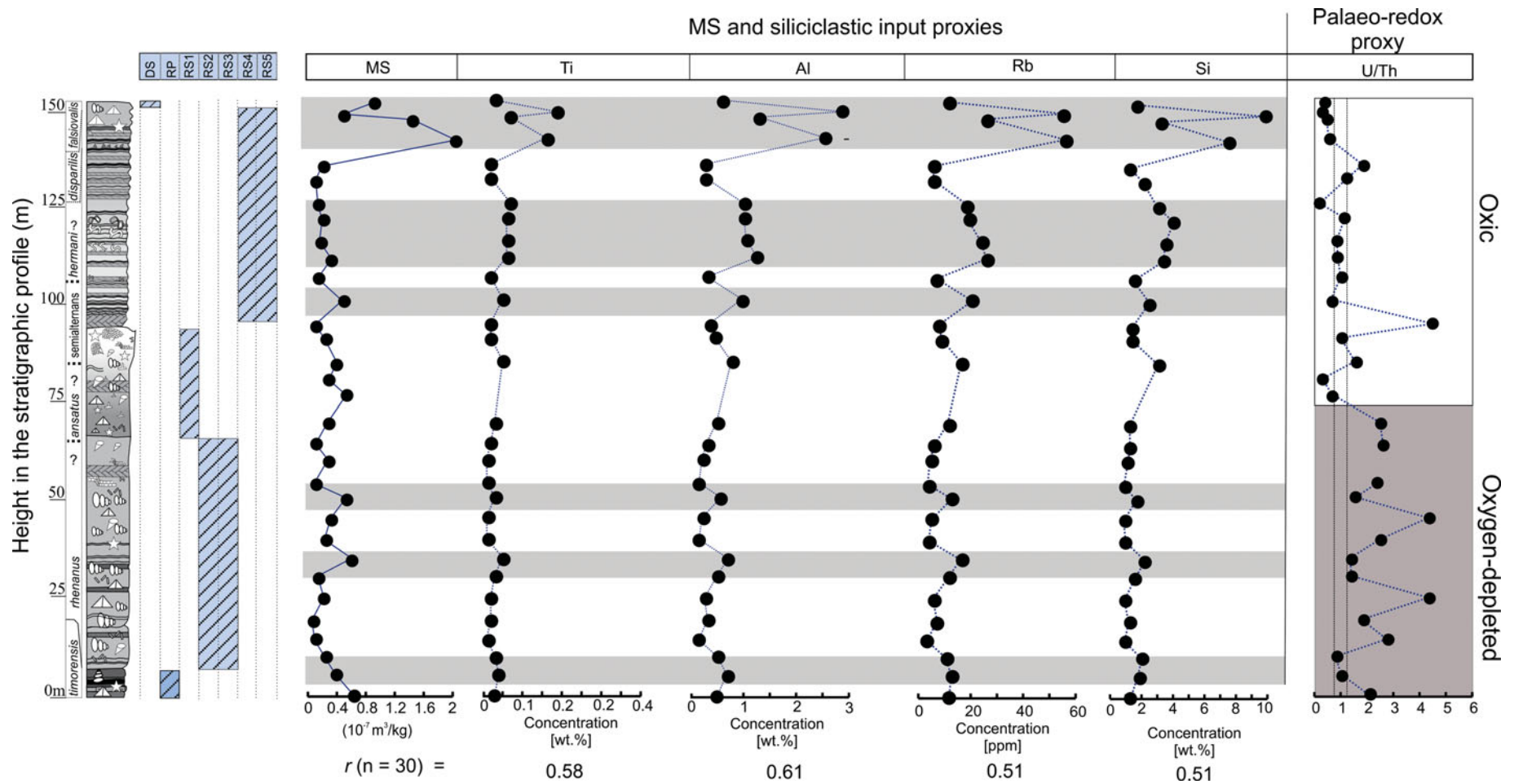


Figure 12. (Colour online) Chemostratigraphic profile of magnetic susceptibility (MS), Ti, Al, Rb, Si and U/Th ratio. Ti, Al and Rb concentrations are considered as proxies for detrital input and show moderate correlation with MS variations. Shaded areas highlight major- or trace-element enrichments. U/Th ratio is considered a proxy for redox condition at the sediment–water interface. Based on the marked drop in U/Th ratio recorded around the mid–late Givetian boundary we subdivided the La Thure section into two parts characterized by different bottom water redox conditions: a lower half with less oxic conditions (shaded area) and an upper half with more oxic conditions. Vertical dotted lines in the U/Th graph represent the threshold values for redox conditions based on Jones & Manning (1994; < 0.75 = oxic, 0.75–1.25 = dysoxic, > 1.25 = anoxic). Main facies belts occurring throughout this section are represented by hatched areas along the lithological log.

et al. 2015), a strong positive correlation ($r = 0.98$) exists between Al and Ti, which means that variations of Al concentration related to diagenetic formation of clay is unlikely. Those observations also mean that, despite the remagnetization event characterizing Devonian limestone in the Ardennes Region (Zegers, Dekkers & Baily, 2003), the main trends in the MS signal still reflect some syn-sedimentary conditions (Da Silva *et al.* 2013). Thus, MS techniques can be used here as a proxy for changes in terrestrial influx driven either by variation in weathering type, reworked source or intensity of this reworking.

5.c.1. Comparison with facies and lithologies

As already demonstrated in various studies (Bábek, Přikryl & Hladil, 2007; Mabillet *et al.* 2008b; Da Silva, Mabillet & Boulvain, 2009; Whalen & Day, 2010; Pas *et al.* 2014), the behaviour of the MS signal classically shows a close relationship with microfacies, indicating an influence of sea-level changes on MS variations. However, the influences of environmental parameters such as water agitation, sedimentation rate, carbonate productivity and siliciclastic supply have already been highlighted as parameters influencing MS changes (Bábek, Přikryl & Hladil, 2007; Mabillet *et al.* 2008b; Da Silva *et al.* 2009, 2013).

The Terres d’Hurs Fm is dominated by mixed carbonate and argillaceous lithologies, which are interpreted to have been deposited in a mid- to distal-ramp setting and assumed to be one of the deepest facies of our succession. This formation (MSU-I) presents high MS values. These results are similar to those obtained in the Belgian Eifelian–Givetian carbonate ramp system. Da Silva, Mabillet & Boulvain (2009) documented a general increase in average MS values from the inner to outer ramp. This increase is explained by the decrease in carbonate productivity with increasing depth and decreasing environmental energy allowing settlement of MS-carrying particles. Data available for the Terres d’Hurs Fm are limited to two microfacies and therefore further consideration of the MS behaviour would be inappropriate.

Sediments characterizing the Mont d’Hurs Fm in the La Thure section mainly represent internal shelf deposition (e.g. facies belt RS2-5, Fig. 9) dominated by relatively pure carbonate as shown by the low values in detrital proxies (Fig. 12). The low mean MS value expressed for this formation (MSU-II) could be related to the high carbonate production in this shallow-water setting within the internal shelf. Here, any input of siliciclastic material that carries magnetic particles will be strongly diluted by carbonate production (Mabillet *et al.* 2008b). The lowermost part of the Fromelennes Fm (Unit 1) has been deposited above the FWB in a biostromal to fore-reef setting (e.g. facies belt RS1, Fig. 9) and records a significant increase in average MS value (MSU-III). In carbonate platform settings, such an increase is commonly attributed to both decreasing water energy level and the lowering of car-

bonate production (e.g. Da Silva, Mabillet & Boulvain, 2009). The transition from fore-reef and biostromal deposits recorded in Unit 1 to the restricted internal platform sediments, belonging to Unit 2 (e.g. facies belt RS4-5), corresponds to a decrease in average MS value (MSU-IVa). This decrease is likely related to water agitation and the confinement characterizing this inter- to supratidal setting, which is dominated by a thick accumulation of laminated mudstone – peloidal grainstone (RS5-LT14). The upper part of Unit 2 was deposited in a relatively similar setting to its lower part. Nevertheless, it records a strong increase in MS values (MSU-IVb). This significant increase in average MS value occurs despite the absence of remarkable deviations in microfacies. Based on a detailed comparison with recent tropical sediment, Boulvain & Pr eat (1986) have demonstrated that during late Givetian time in Belgium (e.g. Fromelennes Fm), shore-face realm depositional processes were mainly dictated by arid conditions similar to those found today in the Persian Gulf. Local occurrences of desiccation cracks and evaporitic crystal-like pseudomorphs (e.g. RS5-LT14–15), indicating arid climate, are also observed in the Givetian La Thure sediments. Since climatic conditions control changes in sediment transport processes we consider that an increase in the aridity on the main landmass (cf. Old Red Sandstone) that bordered the Belgian Givetian carbonate platform might have favoured the amount of wind-related MS-carrying particles transported towards the marine realm. For instance, in a contemporary study dedicated to the evolution of climate during the Mesopotamian Empire (4170 ± 150 yr BP), Cullen *et al.* (2000) performed various mineralogical and geochemical analyses on a marine sediment core from the Gulf of Oman which is downwind of Mesopotamian dust source areas. Their results document a very abrupt increase in aeolian dust parallel to Mesopotamian aridification. This increase in aeolian dust is similarly marked in MS (10^{-6} SI units) and aeolian dolomite (wt%) curves. During Givetian time, evidence of evaporitic plains, semi-arid deserts and continental redbeds are recognized worldwide (Scotese, 2005). Recently Hladil *et al.* (2006) published important gamma-ray spectroscopy (GRS) and MS data obtained in a middle-Eifelian to end-Frasnian Moravian isolated carbonate platform (Czech Republic) and underlined the important role played by aeolian inputs and arid conditions for the MS signal intensity in carbonate rocks. In addition, via the combination of GRS and MS measurements Hladil (2006, fig. 3) showed an increasing amount of atmospheric dust between late Givetian and middle Frasnian time on the Moravian carbonate platform. Therefore, we assume that the significant increase in the MS signal throughout the upper half of the Fromelennes Fm (Unit 2; Fig. 9) could be related to an increase in wind-blown dust deposition in shallow-water triggered by aridification of the main land during middle–late Givetian time. Nevertheless, as mentioned by Sur *et al.* (2010), the geological record of aeolian dust in ancient carbonates is only consistent if

all non-atmospheric sources of silica can be confidently eliminated from consideration (e.g. isolated platform, oceanic basin) for the investigated time interval. This means that only isolated platform or oceanic basin sedimentary records are consistent with such a hypothesis. According to various palaeogeographic reconstructions of Western Europe during Middle Devonian time (Ziegler, 1982; McKerrow & Scotese, 1990) the south of Belgium was located in the immediate vicinity of the Old Red Sandstone continent (e.g. London–Brabant High) and non-atmospheric sources of silica cannot be eliminated. However, to date, siliciclastic facies or riverine deposits have never been identified throughout the upper Givetian in Belgium. Hence, the hypotheses of an increasing MS value related to higher amounts of aeolian-related dust deposition could be envisaged but must be carefully tested, as evidence of the separation of the Belgian platform from the main continent has not been well documented. At present, it is therefore preferable to envisage a combination of aeolian dust and riverine input to explain the recorded MS changes towards late Givetian time within the northwestern margin of the Dinant Basin.

5.d. Palaeoredox conditions within an early–late Givetian platform in the northwestern Dinant Basin

Redox sensitive elemental ratios commonly used to interpret palaeo-oxygenation in bottom water conditions are Ni/Co, V/Cr, V/(V + Ni) and U/Th (Hatch & Leventhal, 1992; Jones & Manning, 1994). The concentrations of the trace elements (Ni, Co, V, and Cr) recorded in our dataset are below the detection limit. The concentrations of U and Th, on the other hand, are within this limit and the calculated redox element ratio U/Th profile through the section is shown in Figure 12. The general evolution of calculated U/Th ratio through the profile can be assigned to the anoxic–dysoxic–oxic threshold values of Jones & Manning (1994; < 0.75 = oxic, 0.75 – 1.25 = dysoxic, > 1.25 = anoxic), although these calculations should be viewed as relative. Indeed, as was mentioned by Rimmer (2004) and other authors (Riquier *et al.* 2005; Śliwiński, Whalen & Jed, 2010), these threshold values should only be used as a relative scale to interpret the degree of palaeo-oxygenation. Subsequently, these threshold values were based either on contemporary dysoxic–anoxic basin analogues or they were developed for a specific palaeobasin. In line with the arguments of Rimmer (2004) and Śliwiński, Whalen & Jed (2010), the evolution of calculated U/Th ratio for the La Thure section reveals a significant large-scale change in the oxygenation level of the sediments (Fig. 12) from oxygen-depleted conditions throughout the lower half of the section to more oxic conditions within the upper half. This lowering in the U/Th ratio is concurrent with the onset of the extensive development of lagoonal–evaporitic settings in the La Thure section (see interval IV in Fig. 10) but also all over the Dinant Basin in Belgium and France (Boulvain & Pr at,

1986). On a more global scale, lagoonal–evaporitic sediments were also recorded in the middle and upper Givetian of the eastern Rheinisches Schiefergebirge (Brilon Reef; Machel, 1990), Harz Mountain (Iberg Reef; Krebs, 1974), Brunai Platform in Czech Republic (Gischler, 1995; Hladil *et al.* 2006) and in the Carnic Alps (Sch onlaub & Histon, 2000). These data support peaks in palaeo-temperature near the onset of Late Devonian time as established by Joachimski *et al.* (2009, 2004) on the basis of a large $\delta^{18}\text{O}$ dataset from biogenic calcite and conodont apatite collected in different locations bordering the Rheic Ocean (see fig. 1 in Joachimski *et al.* 2004). Studying Devonian terrestrial environments, Marshall, Brown & Astin (2011) also highlighted a change to severe aridity towards the end of middle Givetian time, resulting in a major collapse in the terrestrial vegetation. In the La Thure section, the relationship between the depositional setting and the low U/Th ratio value presumably indicates an aridification of the climate as the driving process for the change in bottom water oxygenation. Indeed, the arid climate characterizing middle and late Givetian time may have decreased the amount of organic matter (OM) and nutrients transported seawards. Considering that oxygen dissolved in water is consumed during the decay of OM, a decrease in OM flux towards the marine realm will automatically lead to oxygen enrichment of the bottom water, resulting in oxidizing water conditions. In such conditions, redox sensitive trace metals (e.g. U, V and Mo) are more soluble (Tribovillard *et al.* 2006) and their concentration as well as the U/Th ratio in the sediment–water interface will decrease proportionally.

6. Conclusions

In this paper, we focus on the La Thure section, an outstanding outcrop cutting through a continuous lower to upper Givetian carbonate sequence belonging to the Belgian carbonate platform. About 400 samples were collected from this section and measured for MS, ~200 samples were selected for thin-section analysis and a group of 30 samples was analysed for major- and trace-element concentrations. The major conclusions of this multi-disciplinary investigation are as follows:

(i) Petrographic analyses discerned 18 microfacies which represent a remarkable carbonate platform evolution through early to late Givetian time, ranging from (1) a homoclinal ramp to (2) a discontinuously rimmed shelf and then (3) a drowning shelf. This facies model highlights the fascinating environmental diversity that characterizes a Givetian reefal system within the European Varicides.

(ii) Sedimentary development throughout the section can be divided into five major depositional intervals recording significant sea-level fluctuation and including the Taghanic transgressive event. The drowning that caused the demise of the Belgian Givetian platform is well marked by the re-establishment of open-marine conditions and the subsequent deposition of the overlying lower Frasnian shale.

(iii) A thorough comparison of our sedimentological data with an abundant literature permitted a better understanding of the main facies belt distributions and their evolution within the Dinant Basin for the early–late Givetian interval.

(iv) Based on the moderate to good correlation ($r = 0.51–0.61$; $n = 30$) observed between MS and proxies for siliciclastic influx we can deduce that the magnetic signal is still carrying some primary depositional-induced information. As a result of this, we conclude that MS can serve as a proxy for siliciclastic input variations. Throughout late Givetian time, aeolian-dust related deposition could potentially have had a major influence on the MS signal.

(v) In terms of palaeo-oxygenation, the U/Th proxy indicates an important change in the oxygenation level of bottom water conditions prevailing on the platform, from oxygen-depleted sediments throughout middle Givetian time to more oxic conditions within late Givetian time. This change through more oxic condition is thought to be driven by an increasing aridity towards middle–late Givetian time. Furthermore, we conclude that this hypothesis is concurrent with the increase in palaeo-temperature near the end of middle Givetian time related to the Taghanic Event.

Acknowledgements. This study is a contribution to two UNESCO International Geoscience Programs (IGCP 580 and 596 projects). This work was supported by a Ph.D. fellowship awarded by the Research Foundation–Flanders (FWO) assigned to DDV. J.P. Cullis is acknowledged for the preparation of the large number of thin-sections. This research would not have been possible without the cooperation of the “S.A. carrières de La Thure” which kindly provided access and permission to sample. Marie Coen-Aubert is also warmly thanked for all her helpful answers on biostratigraphic-related queries. Finally, we thank Carlton E. Brett and an anonymous reviewer for their pertinent comments, suggestions and English corrections, which together highly improve the quality of this article.

References

- ABOUSSALAM, Z. S. 2003 Das “Taghanic-Event” im höheren Mittel-Devon von West-Europa und Marokko. *Münster-sche Forschungen zur Geologie und Paläontologie* **97**, 1–332.
- ABOUSSALAM, Z. S. & BECKER, R. T. 2011. The global Taghanic Biocrisis (Givetian) in the eastern Anti-Atlas, Morocco. *Palaeogeography, Palaeoclimatology, Palaeoecology* **304**, 136–64.
- AITKEN, J. D. 1967. Classification and environmental significance of cryptalgal limestones and dolomites, with illustrations from the Cambrian and Ordovician of south-western Alberta. *Journal of Sedimentary Petrology* **37**, 1163–78.
- AVERBUCH, O., TRIBOVILLARD, N., DEVLEESCHOUWER, X., RIQUIER, L., MISTIAEN, B. & VAN VLIET-LANOE, B. 2005. Mountain building-enhanced continental weathering and organic carbon burial as major causes for climatic cooling at the Frasnian–Famennian boundary (c. 376 Ma)? *Terra Nova* **17**, 25–34.
- BÁBEK, O., KALVODA, J., ARETZ, M., COSSEY, P. J., DEVUYST, F. X., HERBIG, H. G. & SEVASTOPULO, G. 2010. The correlation potential of magnetic susceptibility and outcrop gamma-ray logs at Tournaisian–Viséan boundary sections in Western Europe. *Geologica Belgica* **13**, 291–308.
- BÁBEK, O., PŘIKRYL, T. & HLADIL, J. 2007. Progressive drowning of carbonate platform in the Moravo-Silesian Basin (Czech Republic) before the Frasnian/Famennian event: facies, compositional variations and gamma-ray spectrometry. *Facies* **53**, 293–316.
- BACCELLE, L. & BOSELLINI, A. 1965. Diagrammi per la stima visiva della composizione percentuale nelle rocce sedimentarie. *Annali della Università di Ferrara, Sezione IX, Scienze Geologiche e Paleontologiche* **1**(3), 59–62.
- BAIRD, G. C. & BRETT, C. E. 2008. Late Givetian Taghanic bioevents in New York State: new discoveries and questions. *Bulletin of Geosciences* **83**, 357–70.
- BELANGER, I., DELABY, S., DELCAMBRE, B., GHYSEL, P., HENNEBERT, M., LALOUX, M., MARION, J.-M., MOTTEQUIN, B. & PINGOT, J.-L. 2012. Redéfinition des unités structurales du front varisque utilisées dans le cadre de la nouvelle Carte géologique de Wallonie (Belgique). *Geologica Belgica* **15**, 169–75.
- BOULVAIN, F., COEN-AUBERT, M., MANSY, J. L., PROUST, J. N. & TOURNEUR, F. 1995. Le Givetien en Avesnois (Nord de la France): paléoenvironnements et implications paléogéographiques. *Bulletin de la Société belge de Géologie* **103**, 171–203.
- BOULVAIN, F., DA SILVA, A. C., MABILLE, C., HLADIL, J., GERSL, M., KOPTIKOVA, L. & SCHNABL, P. 2010. Magnetic susceptibility correlation of km-thick Eifelian–Frasnian sections (Ardennes and Moravia). *Geologica Belgica* **13**, 309–18.
- BOULVAIN, F., MABILLE, C., POULAIN, G. & DA SILVA, A. C. 2009. Towards a palaeogeographical and sequential framework for the Givetian of Belgium. *Geologica Belgica* **12**, 161–78.
- BOULVAIN, F. & PRÉAT, A. 1986. Les calcaires laminaires du Givétien Supérieur du bord sud du Bassin de Dinant (Belgique, France): témoins d’une évolution paléoclimatique. *Annales de la Société Géologique de Belgique* **109**, 609–19.
- BULTYNCK, P. 1974. Conodontes de la formation de Fromelennes du Givetien de l’Ardenne franco-belge. *Bulletin de l’Institut Royal des Sciences Naturelles de Belgique, Sciences de la Terre* **50** (10), 1–30.
- BULTYNCK, P. 1987. Pelagic and neritic conodont successions from the Givetian of pre-Sahara Morocco and the Ardennes. *Bulletin de l’Institut Royal des Sciences Naturelles de Belgique, Sciences de la Terre* **57**, 149–81.
- BULTYNCK, P., COEN-AUBERT, M., DEJONGHE, L., GODEFROID, J., HANCE, L., LACROIX, D., PRÉAT, A., STAINIER, P., STEEMANS, P., STREEL, M. & TOURNEUR, F. 1991. Les formations du Dévonien moyen de la Belgique. *Mémoires pour Servir à l’Explication des Cartes Géologiques et Minières de la Belgique* **30**, 1–105.
- BULTYNCK, P. & DEJONGHE, L. 2001. Devonian lithostratigraphic units (Belgium). In *Guide to a Revised Lithostratigraphic Scale of Belgium* (eds P. Bultynck & L. Dejonghe), pp. 39–69. Geologica Belgica.
- CASIER, J. G., DEVLEESCHOUWER, X., MAILLET, S., PETITCLERC, E. & PRÉAT, A. 2013. Ostracods and rock facies across the Givetian/Frasnian boundary interval in the Sourd d’Ave section at Ave-et-Auffe (Dinant Synclinorium, Belgium). *Bulletin of Geosciences* **88**, 241–64.
- CASIER, J. G. & PRÉAT, A. 1991. Evolution sédimentaire et Ostracodes de la base du Givetien à Resteigne (bord sud du Bassin de Dinant, Belgique). *Bulletin de l’Institut*

- Royal des Sciences Naturelles de Belgique, Sciences de la Terre* **61**, 157–77.
- CASIER, J. G. & PRÉAT, A. 2013. Ostracodes et lithologie du stratotype de la Formation du Mont d'Hairs (Givetien, Synclinorium de Dinant). *Revue de Paléobiologie* **32**, 481–501.
- COEN-AUBERT, M. 1992. Rugueux coloniaux mésodevoniens du fondry des chiens à nismes (Ardennes, Belgique). *Bulletin de l'Institut Royal des Sciences Naturelles de Belgique, Sciences de la Terre* **62**, 5–21.
- COEN-AUBERT, M. 2000. Stratigraphy and additional rugose corals from the Givetian Mont d'Hairs formation in the Ardennes. *Bulletin de l'Institut Royal des Sciences Naturelles de Belgique, Sciences de la Terre* **70**, 5–24.
- COEN-AUBERT, M. 2002. Temnophyllids and spinophyllids (Rugosa) from the Givetian Mont d'Hairs formation in Belgium. *Bulletin de l'Institut Royal des Sciences Naturelles de Belgique, Sciences de la Terre* **72**, 5–24.
- COEN-AUBERT, M., PRÉAT, A. & TOURNEUR, F. 1986. Compte rendu de l'excursion de la Société belge de Géologie du 6 novembre 1985 consacrée à l'étude du sommet du Couvinien et du Givetien au bord sud du Bassin de Dinant, de Resteigne à Beauraing. *Bulletin de la Société belge de Géologie* **95**, 247–56.
- CULLEN, H. M., DE MENOCAL, P. B., HEMMING, S., BROWN, F. H., GUILDERTSON, T. & SIROCKO, F. 2000. Climate change and the collapse of the Akkadian empire: evidence from the deep sea. *Geology* **28**, 379–82.
- DA SILVA, A. C. & BOULVAIN, F. 2004. From paleosols to carbonate mounds: facies and environments of Middle Frasnian carbonate platform in Belgium. *Geological Quarterly* **48**, 253–66.
- DA SILVA, A. C. & BOULVAIN, F. 2012. Analysis of the Devonian (Frasnian) platform from Belgium: a multi-faceted approach for basin evolution reconstruction. *Basin Research* **24**, 338–56.
- DA SILVA, A. C., DEKKERS, M. J., MABILLE, C. & BOULVAIN, F. 2012. Magnetic susceptibility and its relationship with paleoenvironments, diagenesis and remagnetization: examples from the Devonian carbonates of Belgium. *Studia Geophysica et Geodaetica* **56**, 677–704.
- DA SILVA, A. C., DE VLEESCHOUWER, D., BOULVAIN, F., CLAEYS, P., FAGEL, N., HUMBLET, M., MABILLE, C., MICHEL, J., SARDAR ABADI, M., PAS, D. & DEKKERS, M. J. 2013. Magnetic susceptibility as a high-resolution correlation tool and as a climatic proxy in Paleozoic rocks – merits and pitfalls: examples from the Devonian in Belgium. *Marine and Petroleum Geology* **46**, 173–89.
- DA SILVA, A. C., MABILLE, C. & BOULVAIN, F. 2009. Influence of sedimentary setting on the use of magnetic susceptibility: examples from the Devonian of Belgium. *Sedimentology* **56**, 1292–306.
- DA SILVA, A.-C., POTMA, K., WEISSENBERGER, J. A. W., WHALEN, M. T., HUMBLET, M., MABILLE, C. & BOULVAIN, F. 2009. Magnetic susceptibility evolution and sedimentary environments on carbonate platform sediments and atolls, comparison of the Frasnian from Belgium and Alberta, Canada. *Sedimentary Geology* **214**, 3–18.
- DA SILVA, A. C., WHALEN, M. T., HLADIL, J., KOPTIKOVA, L., CHEN, D., SPASSOV, S., BOULVAIN, F. & DEVLEESCHOUWER, X. 2014. Application of magnetic susceptibility as a paleo-climatic proxy on Paleozoic sedimentary rocks and characterization of magnetic signal – IGCP-580 project and events. *Episodes* **37**, 87–95.
- DE VLEESCHOUWER, D., BOULVAIN, F., DA SILVA, A.-C., PAS, D., LABAYE, C. & CLAEYS, P. 2015. The astronomical calibration of the Givetian (Middle Devonian) timescale (Dinant Synclinorium, Belgium). In *Magnetic Susceptibility Application: A Window onto Ancient Environments and Climate Variations* (eds A. C. Da Silva, M. T. Whalen, J. Hladil, L. Chadimova, D. Chen, S. Spassov, F. Boulvain & X. Devleeschouwer), pp. 245–56. Geological Society of London, Special Publication no. 414.
- DEVLEESCHOUWER, X., PETITCLERC, E., SPASSOV, S. & PRÉAT, A. 2010. The Givetian-Frasnian boundary at Nismes parastratotype (Belgium): the magnetic susceptibility signal controlled by ferromagnetic minerals. *Geologica Belgica* **13**, 351–66.
- DICKSON, J. A. D. 1965. A modified staining technique for carbonates in thin section. *Nature* **205**(4971), 587.
- DUNHAM, R. J. 1962. Classification of carbonate rocks according to depositional texture. In *Classification of Carbonate Rocks* (ed. W. E. Ham), pp. 108–21. American Association of Petroleum Geologists Memoir.
- EMBRY, A. F. & KLOVAN, J. E. 1972. Absolute water depth limits of Late Devonian paleoecological zones. *Geologische Rundschau* **61**, 672–86.
- ERRERA, M., MAMET, B. & SARTENAER, P. 1972. Le calcaire Givetien à Givet. *Bulletin de l'Institut Royal des Sciences Naturelles de Belgique, Science de la Terre* **48**, 1–59.
- FLÜGEL, E. 2004. *Microfacies Analysis of Carbonate Rocks. Analysis, Interpretation and Application*. Berlin: Springer-Verlag.
- FÜRSICH, F. T. & OSCHMANN, W. 1993. Shell beds as tools in basin analysis: the Jurassic of Kachchh, western India. *Journal of the Geological Society, London* **150**, 169–85.
- FÜRSICH, F. T. & PANDEY, D. K. 1999. Genesis and environmental significance of Upper Cretaceous shell concentrations from the Cauvery Basin, southern India. *Palaeogeography, Palaeoclimatology, Palaeoecology* **145**, 119–39.
- GARLAND, J., TUCKER, M. E. & SCRUTTON, C. T. 1996. Microfacies analysis and metre-scale cyclicity in the Givetian back-reef sediments of southeast Devon. *Proceedings of the Ussher Society* **9**, 31–6.
- GISCHLER, E. 1995. Current and wind induced facies patterns in a Devonian atoll; Iberg Reef, Harz Mts., Germany. *Palaios* **10**, 180–9.
- GOUWY, S. & BULTYNCK, P. 2003. Conodont based graphic correlation of the Middle Devonian formations of the Ardenne (Belgium): implications for stratigraphy and construction of a regional composite. *Revista Española de Micropaleontología* **35**, 315–44.
- HATCH, J. R. & LEVENTHAL, J. S. 1992. Relationship between inferred redox potential of the depositional environment and geochemistry of the Upper Pennsylvanian (Missourian) Stark Shale Member of the Dennis Limestone, Wabaunsee County, Kansas, U.S.A. *Chemical Geology* **99**, 65–82.
- HENNEBERT, M. 2008. *Carte Géologique de Wallonie, Merbes-Le-Château – Thuin n° 52/1-2, à 1/25000 et sa Notice Explicative*. Ministère de la région Wallonne.
- HLADIL, J., GERSL, M., STRNAD, L., FRANA, J., LANGROVA, A. & SPISIAK, J. 2006. Stratigraphic variation of complex impurities in platform limestones and possible significance of atmospheric dust: a study with emphasis on gamma-ray spectrometry and magnetic susceptibility outcrop logging (Eifelian–Frasnian, Moravia, Czech Republic). *International Journal of Earth Sciences* **95**, 703–23.
- HOUSE, M. R. 2002. Strength, timing, setting and cause of mid-Palaeozoic extinctions. *Palaeogeography, Palaeoclimatology, Palaeoecology* **181**, 5–25.

- JOACHIMSKI, M. M., BREISIG, S., BUGGISCH, W., TALENT, J. A., MAWSON, R., GEREKE, M., MORROW, J. R., DAY, J. & WEDDIGE, K. 2009. Devonian climate and reef evolution: insights from oxygen isotopes in apatite. *Earth and Planetary Science Letters* **284**, 599–609.
- JOACHIMSKI, M. M., VAN GELDERN, R., BREISIG, S., BUGGISCH, W. & DAY, J. 2004. Oxygen isotope evolution of biogenic calcite and apatite during the Middle and Late Devonian. *International Journal of Earth Sciences* **93**, 542–53.
- JONES, B. & MANNING, D. A. C. 1994. Comparison of geochemical indices used for the interpretation of palaeoredox conditions in ancient mudstones. *Chemical Geology* **111**, 111–29.
- JOHNSON, J. G. 1970. Taghanic onlap and the end of North American Devonian provinciality. *Geological Society of America Bulletin* **81**, 2077–106.
- JOHNSON, J. G., KLAPPER, G. & SANDBERG, C. A. 1985. Devonian eustatic fluctuations in Euramerica. *Geological Society of America Bulletin* **96**, 567–87.
- KIDWELL, S. M. & BOSENCE, D. W. 1991. Taphonomy and time-averaging of marine shelly faunas. In *Taphonomy: Releasing the Data Locked in the Fossil Record* (eds P. A. Allison & D. E. G. Briggs), pp. 115–209. New York: Plenum Press.
- KIESSLING, W., FLÜGEL, E. & GOLONKA, J. A. N. 2003. Patterns of Phanerozoic carbonate platform sedimentation. *Lethaia* **36**, 195–225.
- KOPIKOVÁ, L. 2011. Precise position of the Basal Choteč event and evolution of sedimentary environments near the Lower–Middle Devonian boundary: the magnetic susceptibility, gamma-ray spectrometric, lithological, and geochemical record of the Prague Synform (Czech Republic). *Palaeogeography, Palaeoclimatology, Palaeoecology* **304**, 96–112.
- KOPIKOVÁ, L., BÁBEK, O., HLADIL, J., KALVODA, J. & SLAVÍK, L. 2010. Stratigraphic significance and resolution of spectral reflectance logs in Lower Devonian carbonates of the Barrandian area, Czech Republic; a correlation with magnetic susceptibility and gamma-ray logs. *Sedimentary Geology* **225**, 83–98.
- KREBS, W. 1974. Devonian carbonate complexes of Central Europe. In *Reefs in Time and Space: Selected Examples from the Recent and Ancient* (ed. L. F. Laporte), pp. 155–208. Special Publication of the Society for Economic Paleontologists and Mineralogists.
- LECOMPTE, M. 1951. Les stromatoporoides du Dévonien moyen et supérieur du Bassin de Dinant: première partie. *Mémoires de l'Institut Royal des Sciences Naturelles de Belgique* **116**, 1–215.
- LECOMPTE, M. 1952. Les stromatoporoides du Dévonien moyen et supérieur du bassin de Dinant: deuxième partie. *Mémoires de l'Institut Royal des Sciences Naturelles de Belgique* **117**, 216–359.
- LOGAN, B. V. & SEMENUK, V. 1976. *Dynamic Metamorphism: Processes and Products in Devonian Carbonate Rocks, Canning Basin, Western Australia*. Special Publication of the Geological Society of Australia **6**, 138 pp.
- MABILLE, C., DE WILDE, C., HUBERT, B., BOULVAIN, F. & DA SILVA, A. C. 2008a. Detailed sedimentological study of a non-classical succession for Trois-Fontaines and Terres d'Haurs formations (Lower Givetian, Marenne, Belgium) – introduction to the Marenne Member. *Geologica Belgica* **11**, 217–38.
- MABILLE, C., PAS, D., ARETZ, M., BOULVAIN, F., SCHRÖDER, S. & SILVA, A. C. 2008b. Deposition within the vicinity of the Mid-Eifelian High: detailed sedimentological study and magnetic susceptibility of a mixed ramp-related system from the Eifelian Lauch and Nohn formations (Devonian; Ohlesberg, Eifel, Germany). *Facies* **54**, 597–612.
- MACHEL, H. G. 1990. Faziesinterpretation des Briloner Riffs mit Hilfe eines Faziesmodells für devonische Rifffarbonate. *Geologische Jahrbuch Reihe D* **95**, 43–83.
- MAILLET, S., MILHAU, B. & DOJEN, C. 2013. Stratigraphical distribution of Givetian ostracods in the type-area of the Fromelennes Formation (Fromelennes, Ardennes, France) and their relationship to global event. *Bulletin of Geosciences* **88**, 865–92.
- MAILLET, S., MILHAU, B. & PINTE, E. 2011. The Fromelennes Formation in the type-area (Fromelennes, Ardennes, France). *Annales de la Société Géologique du Nord* **18**, 9–34.
- MAMET, B. L. 1970. Sur les Umbellaceae. *Canadian Journal of Earth Sciences* **7**, 1164–71.
- MAMET, B. 1991. Carboniferous calcareous algae. In *Calcareous Algae and Stromatolites* (ed. R. Rober), pp. 370–451. Berlin, Heidelberg: Springer.
- MAMET, B. & PRÉAT, A. 1986. Algues givetiennes du bord sud du bassin de Dinant et des régions limitrophes. *Annales de la Société Géologique de Belgique* **109**, 431–54.
- MARSHALL, J. E. A., BROWN, J. F. & ASTIN, T. R. 2011. Recognising the Taghanic Crisis in the Devonian terrestrial environment and its implications for understanding land-sea interactions. *Palaeogeography, Palaeoclimatology, Palaeoecology* **304**, 165–83.
- MCKERROW, W. S. & SCOTSE, C. R. (eds) 1990. *Paleozoic Palaeogeography and Biogeography*. Geological Society of London, Memoir no. 12.
- MICHEL, J., BOULVAIN, F., PHILIPPO, S. & DA SILVA, A. C. 2010. Palaeoenvironmental study and small scale correlations using facies analysis and magnetic susceptibility of the mid-Emsian (Himmelbaach Quarry, Luxembourg). *Geologica Belgica* **13**, 447–58.
- MOLINA GARZA, R. S. & ZIJDERVELD, J. D. A. 1996. Paleomagnetism of Paleozoic strata, Brabant and Ardennes Massifs, Belgium: implications of pre-folding and post-folding Late Carboniferous secondary magnetizations for European apparent polar wander. *Journal of Geophysical Research B: Solid Earth* **101**, 15799–818.
- NARKIEWICZ, K., NARKIEWICZ, M. & BULTYNCK, P. 2015. Conodont biofacies of the Taghanic transgressive interval (middle Givetian): Polish record and global comparisons. In *Devonian Climate, Sea Level and Evolutionary Events* (eds R. T. Becker, P. Königshof & C. E. Brett). Geological Society of London, Special Publication no. 423.
- NEUMANN, M., POZARYSKA, K. & VACHARD, D. 1975. Remarques sur les microfacies du Dévonien de Lublin (Pologne). *Revue de Micropaleontologie* **18**, 38–52.
- PAS, D., DA SILVA, A. C., CORNET, P., BULTYNCK, P., KÖNIGSHOF, P. & BOULVAIN, F. 2013. Sedimentary development of a continuous Middle Devonian to Mississippian section from the fore-reef fringe of the Brilon Reef Complex (Rheinisches Schiefergebirge, Germany). *Facies* **59**, 969–90.
- PAS, D., DA SILVA, A. C., DEVLEESCHOUWER, X., DE VLEESCHOUWER, D., LABAYE, C., CORNET, P., MICHEL, J. & BOULVAIN, F. 2015. Sedimentary development and magnetic susceptibility evolution of the Frasnian in Western Belgium (Dinant Synclinorium, La Thure section). In *Magnetic Susceptibility Application: A Window onto Ancient Environments and Climatic Variations* (eds A. C. Da Silva, M. T. Whalen, J. Hladil, L. Chadimova, D. Chen, S. Spassov, F. Boulvain & X. Devleeschouwer),

- pp. 15–36. Geological Society of London, Special Publication no. 414.
- PAS, D., DA SILVA, A. C., SUTTNER, T., KIDO, E., BULTYNCK, P., PONDRELLI, M., CORRADINI, C., DE VLEESCHOUWER, D., DOJEN, C. & BOULVAIN, F. 2014. Insight into the development of a carbonate platform through a multi-disciplinary approach: a case study from the Upper Devonian slope deposits of Mount Freikofel (Carnic Alps, Austria/Italy). *International Journal of Earth Sciences* **103**, 519–38.
- PETTIJOHN, F. J., POTTER, P. N. & SIEVER, R. 1972. *Sand and Sandstone*. Berlin: Springer.
- PLAYFORD, P. E. 1980. Devonian “Great Barrier Reef” of Canning Basin, Western Australia. *American Association of Petroleum Geologists Bulletin* **64**, 814–40.
- POHLER, S. M. L. 1998. Devonian carbonate buildup facies in an intra-oceanic island arc (Tamworth Belt, New South Wales, Australia). *Facies* **39**, 1–34.
- PRÉAT, A. 2006. Le Givétien franco-belge: moteur de la sédimentation eustatique vs subsidence? *Géologie de la France* **1–2**, 45–51.
- PRÉAT, A. & BOULVAIN, F. 1982. Etude sédimentologique des calcaires givétiens à Vaucelles (bord Sud du Synclinorium de Dinant). *Annales de la Société Géologique de Belgique* **105**, 273–82.
- PRÉAT, A. & BOULVAIN, F. 1988. Middle and upper Devonian carbonate platform evolution in Dinant and Namur Basins (Belgium, France). In *Excursion A-1, IAS 9th European Regional Meeting: Excursion Guidebook*, pp. 1–25.
- PRÉAT, A. & BULTYNCK, P. 2006. Givetian. In *Chronostratigraphic Units Named from Belgium* (eds P. Bultynck & L. Dejonghe), pp. 9–18. Geologica Belgica.
- PRÉAT, A. & CARLIEZ, D. 1994. Microfaciès et cyclicité dans le Givetien supérieur de Fromelennes (Synclinorium de Dinant, France). *Annales de la Société Géologique de Belgique* **117**, 227–43.
- PRÉAT, A., CEULENEER, G. & BOULVAIN, F. 1987. Etude sédimentologique des calcaires du Givétien Inférieur d’Olloy-sur-Viroin (bord Sud du Bassin de Dinant, Belgique). *Annales de la Société Géologique du Nord* **106**, 251–65.
- PRÉAT, A., COEN-AUBERT, M., MAMET, B. & TOURNEUR, F. 1984. Sédimentologie et paléocéologie de trois niveaux récifaux du Givétien inférieur de Resteigne (bord sud du Bassin de Dinant, Belgique). *Bulletin de la Société belge de Géologie* **93**, 227–40.
- PRÉAT, A. & KASIMI, R. 1995. Sédimentation de rampe mixte silico-carbonatée des couches de transition eiféliennes-givétiennes franco-belge. Deuxième partie: cyclostratigraphie et paléostraturation. *Bulletin des Centres de Recherches et d’Exploration-Production. Elf-Aquitaine* **19**, 329–75.
- PRÉAT, A. & MAMET, B. 1989. Sédimentation de la plateforme carbonatée Givétienne Franco-belge. *Bulletin des Centres de Recherches et d’Exploration-Production. Elf-Aquitaine* **13**, 47–86.
- PURSER, B. H. 1980. *Sédimentation et Diagenèse des Carbonates Néritiques Récents*. Paris: Edition Technip.
- READ, J. F. 1985. Carbonate platform facies models. *American Association of Petroleum Geologists Bulletin* **69**, 1–21.
- RIMMER, S. M. 2004. Geochemical paleoredox indicators in Devonian–Mississippian black shales, Central Appalachian Basin (USA). *Chemical Geology* **206**, 373–91.
- RQUIER, L., AVERBUCH, O., DEVLEESCHOUWER, X. & TRIBOVILLARD, N. 2010. Diagenetic versus detrital origin of the magnetic susceptibility variations in some carbonate Frasnian–Famennian boundary sections from Northern Africa and Western Europe: Implications for paleoenvironmental reconstructions. *International Journal of Earth Sciences* **99** (Suppl. 1), 57–73.
- RQUIER, L., TRIBOVILLARD, N., AVERBUCH, O., JOACHIMSKI, M. M., RACKI, G., DEVLEESCHOUWER, X., EL ALBANI, A. & RIBOULLEAU, A. 2005. Chapter 8: Productivity and bottom water redox conditions at the Frasnian–Famennian boundary on both sides of the Eovariscan Belt: constraints from trace-element geochemistry. In *Understanding Late Devonian and Permian-Triassic Biotic and Climatic Events* (eds J. Over, J. Morrow & P. Wignall), pp. 199–224. Developments in Palaeontology and Stratigraphy 20. Elsevier.
- SCHOLLE, P. A. & ULMER-SCHOLLE, D. S. 2003. *Color Guide to the Petrography of Carbonate Rocks: Grains, Texture, Porosity, Diagenesis*. American Association of Petroleum Geologist Memoir 77.
- SCHÖNLAUB, H. P. & HISTON, K. 2000. The Palaeozoic evolution of the Southern Alps. *Mitteilungen der Österreichischen Geologischen Gesellschaft* **92** (1999), 15–34.
- SCOTESE, C. R. 2005. Paleomap Project, Climate History. <http://www.scotese.com/climate.htm>
- SKOMPSKI, S. & SZULCZEWSKI, M. 1994. Tide-dominated Middle Devonian sequence from the northern part of the Holy Cross Mountains (Central Poland). *Facies* **30**, 247–65.
- ŚLIWIŃSKI, M. G., WHALEN, M. T. & JED, D. 2010. Trace element variations in the middle Frasnian *punctata* zone (Late Devonian) in the Western Canada sedimentary basin – changes in oceanic bioproductivity and paleoredox spurred by a pulse of terrestrial afforestation? *Geologica Belgica* **13**, 459–82.
- ŚLIWIŃSKI, M. G., WHALEN, M. T., MEYER, F. J. & MAJS, F. 2012. Constraining clastic input controls on magnetic susceptibility and trace element anomalies during the Late Devonian *punctata* Event in the Western Canada Sedimentary Basin. *Terra Nova* **24**, 301–9.
- STRASSER, A. 1986. Ooids in Purbeck limestones (lowermost Cretaceous) of the Swiss and French Jura. *Sedimentology* **33**, 711–27.
- SUR, S., SOREGHAN, M. J., SOREGHAN, G. S. & STAGNER, A. F. 2010. Extracting the silicate mineral fraction from ancient carbonate: assessing the geologic record of dust. *Journal of Sedimentary Research* **80**, 763–9.
- TORSVIK, T. H., VAN DER VOO, R., PREEDEN, U., NIOCAILL, C. M., STEINBERGER, B., DOUBROVINE, P. V., VAN HINSBERGEN, D. J. J., DOMEIER, M., GAINA, C., TOHVER, E., MEERT, J. G., MCCAUSLAND, P. J. & COCKS, L. R. M. 2012. Phanerozoic polar wander, palaeogeography and dynamics. *Earth-Science Reviews* **114**, 325–68.
- TRIBOVILLARD, N., ALGEO, T. J., LYONS, T. & RIBOULLEAU, A. 2006. Trace metals as paleoredox and paleoproductivity proxies: an update. *Chemical Geology* **232**, 12–32.
- TUCKER, M. E. 2001. *Sedimentary Petrology. An introduction to the Origin of the Sedimentary Rocks, 3rd Edition*. London: Blackwell.
- WHALEN, M. T. & DAY, J. E. 2008. Magnetic susceptibility, biostratigraphy, and sequence stratigraphy: insights into Devonian carbonate platform development and basin infilling, western Alberta, Canada. *Society for Sedimentary Geology* **89**, 291–314.
- WHALEN, M. T. & DAY, J. E. 2010. Cross-basin variations in magnetic susceptibility influenced by changing sea level, paleogeography, and paleoclimate: Upper

- Devonian, western Canada sedimentary basin. *Journal of Sedimentary Research* **80**, 1109–27.
- WILSON, J. L. 1975. *Carbonate Facies in Geologic History*. Berlin, Heidelberg, New York: Springer-Verlag.
- WOOD, R. 2000. Palaeoecology of a Late Devonian back reef: Canning Basin, Western Australia. *Palaeontology* **43**, 671–703.
- ZEGERS, T. E., DEKKERS, M. J. & BAILY, S. 2003. Late Carboniferous to Permian remagnetization of Devonian limestones in the Ardennes: role of temperature, fluids, and deformation. *Journal of Geophysical Research* **108**(B7), 5/1–5/19.
- ZIEGLER, A. P. 1982. *Geological Atlas of Western and Central Europe*. The Hague: Shell Internationale Petroleum Maatschappij B.V.
- ZWING, A., MATZKA, J., BACHTADSE, V. & SOFFEL, H. C. 2005. Rock magnetic properties of remagnetized Palaeozoic clastic and carbonate rocks from the NE Rhenish massif, Germany. *Geophysical Journal International* **160**, 477–86.